This article has been accepted for publication in IEEE Internet of Things Journal. This is the author's version which has not been fully edited and content may change prior to final publication. Citation information: DOI 10.1109/JIOT.2024.3364756

Best Response Dynamics Convergence for Generalised Nash Equilibrium Problems: an Opportunity for Autonomous Multiple Access Design in Federated Learning

Guillaume Thiran, *Member, IEEE,* Ivan Stupia, *Member, IEEE,* and Luc Vandendorpe, *Fellow, IEEE*

***Abstract*—Federated learning is envisioned to be a key enabler of network functionalities based on artificial intelligence. Multiple access mechanisms supporting the learning task must then be designed, in order to provide an efficient interplay between the communication and computation resources.**

This work considers thus a multi-level slotted random access scheme autonomously optimised by each node. Due to their mutual coupling, the nodes' interaction is an instance of the Best Response Dynamics (BRD) of a Generalised Nash Equilibrium Problem (GNEP). Within this framework, levers are identified, guaranteeing the convergence of the interactions to an equilibrium point at which the federated learning task is supported. These levers, on which the network manager can act, are validated by numerical simulations. These latter moreover show that the performance loss due to the autonomous character of the nodes is negligible with respect to the result of a centralised optimisation.

On a broader mathematical level, this work defines a class of GNEPs for which sufficient convergence conditions for the totally asynchronous BRD are obtained. The considered class, named the GNEPs with polyhedral strategy sets and variable right-hand sides, encompasses a wide variety of GNEPs, and in particular GNEPs which are neither jointly convex nor generalised potential games. The obtained conditions depend on the first and second derivatives of the objective and constraint functions, and they constitute thus an off-the-shelf framework to study the BRD of GNEPs belonging to the identified class.

***Index Terms*—Federated learning, Multiple access, Game Theory, Generalised Nash Equilibrium Problem, Best Response Dynamics, Convergence**

I. Introduction

With the development of functionalities based on artificial intelligence and machine learning, wireless networks will have to support the learning processes of many applications. While alleviating the computational burden, cloud-based implementations require gathering the local information of all nodes, leading to a heavy communication load. Thus, the framework of Federated Learning (FL) [1] has been developed, in which the model underlying a distributed dataset is iteratively inferred. Each iteration starts with the server broadcasting the current global model to the nodes, named the workers. Then, each worker locally updates the model, and sends back the updated model to the server. Finally, the updated local models are aggregated into a new global model. Such procedure enables to preserve the private character of the nodes' datasets. However, spectrum scarcity, and the limited computational capabilities of the devices, call for an optimisation of the utilisation of the communication and computation resources [2].

The resource allocations of different workers are however coupled, either by the shared communication resources, or by the FL requirements. By jointly considering all workers, centralised optimisation algorithms enable to reach a global optimum. Nevertheless, they require gathering the optimisation information into a unique node, and this thus contradicts the privacy-preserving character of FL. To avoid this, methods which leave both the computation and the information to the workers seem adequate. The framework of Game Theory (GT) is therefore particularly relevant, as it considers the nodes as the decision-makers [3]. In such setting, the challenge moves from solving a complicated optimisation problem, to the analysis of the interactions occurring between the workers. More precisely, one must ensure the workers find a point at which no worker has an interest in changing its resource allocation, such stable point being named an equilibrium. When the equilibrium is reached iteratively, the sequence of resource allocation profiles occurring between the initial profile and the equilibrium point is named the game dynamics. One of the most straightforward dynamics is the Best Response Dynamics (BRD), which lets each worker iteratively update its resource profile in order to optimise its own local performance. Due to its simplicity, the BRD is of great interest in wireless scenarios, and obtaining convergence guarantees is therefore critical.

Owing to the FL requirements, the workers' optimisation problems are however coupled both through the objective and constraint functions. The resulting interactions are thus an instance of a Generalised Nash Equilibrium Problem (GNEP) [4], as opposed to traditional Nash equilibrium problems. To the authors' knowledge, obtaining convergence guarantees for the BRD of a GNEP, and applying these to an FL problem, is however an unsolved problem. This paper provides thus i) a framework to obtain convergence guarantees for the BRD of GNEP, and ii) an analysis of the convergence conditions

G. Thiran, I. Stupia and L. Vandendorpe are with the ELectrical ENgineering department (ELEN), Université Catholique de Louvain (UCLouvain), Louvain-la-Neuve, 1348, Belgium, e-mail: {guillaume.thiran, ivan.stupia, luc.vandendorpe}@uclouvain.be.

Guillaume Thiran is a Research Fellow of the Fonds de la Recherche Scientifique – FNRS.

Copyright (c) 20xx IEEE. Personal use of this material is permitted. However, permission to use this material for any other purposes must be obtained from the IEEE by sending a request to pubs-permissions@ieee.org.

© 2024 IEEE. Personal use is permitted, but republication/redistribution requires IEEE permission. See https://www.ieee.org/publications/rights/index.html for more information.

This article has been accepted for publication in IEEE Internet of Things Journal. This is the author's version which has not been fully edited and content may change prior to final publication. Citation information: DOI 10.1109/JIOT.2024.3364756

associated with an FL scheme. As this work brings together elements from wireless networks, FL and GT, the terms *node*, *worker*, and *player* will be used interchangeably below.

A. Related Works

a) FL resource allocation: Resource allocation for FL tackles the problem of allocating the computation and communication resources to optimise the FL performance. The performance metrics are among others the accuracy of the trained model, the training latency, the energy consumption or the privacy [5]. To that aim, literature provides models linking the training accuracy to the number and quality of learning iterations, which can then be connected to the time, computation and energy consumption [6], [7]. With such links, performance optimisation can be performed, for instance to optimise the energy and latency [8]–[12], the learning error [13], [14], the communication success probability [15] or privacy [16]. However, the above works consider centralised schemes, for which the required side-information exchange can be an issue.

Instead, workers can be considered as autonomous and competitive, and their interaction must then be studied within the GT framework [17]. This framework has for instance been used in order to properly design incentive mechanisms pushing the devices to participate in the learning process [18], [19], and preventing them from acquiring the model without actively participating in the learning task [20]. Still in a GT perspective, the models developed in [21], [22] show that workers are not only coupled through their objective functions, but also through their constraints. Indeed, since FL updates must wait for all active workers, each worker has typically latency constraints which depend on the action of the others. Instead of a classical Nash equilibrium problem, such constraint coupling makes it an instance of a GNEP [4]. The benefit of considering a GT approach is that it naturally captures the delocalised and autonomous characteristics of the network, by considering the workers as the decision-makers.

In this autonomy perspective, the multiple access mechanisms envisioned for FL must be discussed. Dynamically adapting the resource allocation plan of an orthogonal access scheme to the workers' needs would require lots of side-information exchanges. Avoiding this, Random Access (RA) mechanisms [23] let the nodes communicate sporadically and adaptively on a shared communication resource. In RA mechanisms, at a given time, each node has some probability to try to transmit information to the access point. This probability, named the access probability or the communication probability, impacts not only the considered node, but also the others since they all share the same resource. The access point may then receive nothing, receive the communication from one node, or from several nodes simultaneously. In this third case, a collision is said to occur, which usually results in the access point being unable to decode any of the communications. Thanks to their uncoordinated character, RA schemes are envisioned as a key enabler of Machine-Type Communications (MTCs), in which many nodes communicate with a server [24]–[26]. As the communication decisions belong to the nodes and not to a central authority, such protocols indeed adapt very well to a change of the communicating nodes, and efficiently scale with their number. Such MTC setting precisely occurs during the uplink communication step of FL, when the workers transmit their updated model to the server. RA schemes have thus been considered for FL, such as Carrier Sensing Multiple Access (CSMA) [27], ALOHA [28] and Multi-Channel ALOHA [29]–[32]. In such schemes, optimising the protocol parameters to mitigate the rate loss due to the collisions is nevertheless critical [24], [27], [30]. As discussed above, this access optimisation depends on the parameters of the other nodes. Instead of performing a centralised optimisation, coupling a RA mechanism with a GNEP approach enables to design a fully autonomous FL process with both the resource allocation and the access optimisation performed locally at each node. Yet, to the authors' knowledge, such perspective has not yet been considered in the literature.

b) Algorithms for GNEPs: The study of GNEPs dates back to the works of Debreu [33], [34], in which the problem was known as an abstract economy problem. Since then, many properties of the equilibrium points (existence, uniqueness, stability) as well as algorithms enabling to find such equilibria have been studied [4], [35], [36]. Most of these algorithms are based on reformulations of a GNEP into an equivalent problem, which can then be solved using tailored, centralised methods [37]–[42]. It should be noted that a particular class of GNEPs, named the jointly convex GNEPs, benefits from stronger equivalences and simpler algorithms. This class is characterised by the fact that the shared constraints are convex, and identical for all players.

As they are centralised, the above algorithms require to gather the players' information into a unique node, and then to communicate back the obtained equilibrium point. These algorithms are consequently not suited to scenarios in which side-information exchanges are an issue, as it is the case in this paper. Hence, schemes which let both the information and the computation localised into the players must be considered, being named decomposition methods in the GT literature. To that aim, the equilibria of a GNEP can be obtained by solving a sequence of classical Nash equilibrium problems [43]. If the algorithm used to solve these latter can be decomposed, then the GNEP algorithm is an instance of a decomposition method. More recently, in [44], [45], decomposition methods based on projection and proximal operators have been shown to converge to an equilibrium.

While avoiding the sharing of players local information, the above methods are still demanding in terms of computations and convergence speed. They involve multi-layer loops, in which the inner loop solves parametrised problems till convergence, while the outer loop updates the parameters in order to drift towards an equilibrium. Additionally, coordination is still required in order to synchronise the loops entrance and exit. The BRD, being a decomposition method, alleviates these problems, especially when the players' updates are asynchronous. For some specific instances of GNEPs, BRD convergence guarantees have been obtained using ad-hoc arguments [46]–[48]. However, as the developments are specific to the considered scenarios, they cannot be applied to other

© 2024 IEEE. Personal use is permitted, but republication/redistribution requires IEEE permission. See https://www.ieee.org/publications/rights/index.html for more information.

This article has been accepted for publication in IEEE Internet of Things Journal. This is the author's version which has not been fully edited and content may change prior to final publication. Citation information: DOI 10.1109/JIOT.2024.3364756

problems. For the class of the generalised potential games, a particular class of GNEPs, convergence of a regularised version of the BRD can be ensured [49], [50]. This class, characterised by the fact that all players implicitly optimise a unique potential function, is nevertheless quite peculiar.

However, there currently exists no theoretical convergence guarantees for the BRD of general GNEPs. Practice has shown it often reaches an equilibrium [4], but counterexamples have also been exhibited [49]. This gap between theory and practice calls thus for conditions delimiting GNEPs for which BRD convergence is ensured.

B. Contributions

Filling the above gaps, this paper contributes to the two-fold goal of i) on the applicative level, designing and analysing a fully autonomous multiple access scheme supporting an FL algorithm, and ii) on a broader mathematical level, providing convergence conditions for the BRD of GNEPs.

For the FL, the detailed contributions are as follows.

- An autonomous slotted multi-level random access mechanism is developed, in which each worker locally designs its access probabilities so as to support the FL task.
- Conditions on the convergence of the RA probabilities towards an equilibrium are obtained, enabling to extract levers instrumental to the control of the workers' interactions. These levers are validated numerically, showing that convergence can be ensured with high probability, even with many workers and high accuracies.
- The workers' performance at the equilibrium is numerically compared to the one achieved when performing a joint, centralised optimisation across all workers. This comparison shows that the loss due to the autonomous worker behaviour is negligible.

For the BRD of GNEPs, this paper provides the following.

- A class of GNEPs, named the GNEPs with polyhedral strategy sets and variable Right-Hand Sides (RHSs), is delimited. Beside standard convexity and differentiability assumptions, this class is characterised by the fact that the constraints of each player must be linear in its own variables, with a possibly nonlinear dependence in the other players' variables limited to the RHS term.
- For this class, sufficient convergence conditions for the totally asynchronous BRD are obtained. These conditions depend on the first and second derivatives of the objective and constraint functions. They thus constitute an off-the-shelf framework to study the BRD of GNEPs belonging to the delimited class.

C. Organisation

This paper is structured as follows. First, in Section II, the FL scenario is described, and the coupled optimisation problems of the devices are formulated. Then, Section III defines the class of GNEPs with polyhedral strategy set and variable RHSs, and Section IV provides the sufficient convergence conditions for the BRD convergence. The developed tools are finally applied to the FL problem in Section V, and they are validated numerically.

D. Notations

Scalars are written as normal letters: a or A, column vectors as boldface lower-case ones: $\mathbf{a} = [a_1, \ldots, a_n]^\top = [a_i]_{i=1}^n$, matrices as boldface upper-case ones: $\mathbf{A}$, and sets with calligraphic letters: $\mathcal{A} = \{a_1, \ldots, a_n\} = \{a_i\}_{i=1}^n$. Vector and matrix elements can also be indexed as $[\mathbf{a}]_i$ and $[\mathbf{A}]_{ij}$. The notation $\mathbf{a}_{-i}$ denotes the same vector as $\mathbf{a}$, without the ith element. The size-n identity matrix is written as $\mathbf{I}_n$, the full-zero vector and matrix as $\mathbf{0}_n$ and $\mathbf{0}_{m\times n}$ and the full-one vector as $\mathbf{1}_n$. When it is clear from the context, the size indices are made implicit. For a vector $\mathbf{a}$, $\|\mathbf{a}\|$ is a generic notation for any vector norm, while its 2-norm is denoted as $\|\mathbf{a}\|_2$. $\mathrm{Diag}(\mathbf{a})$ refers to the diagonal matrix $\mathbf{A}$ with diagonal elements $A_{ii} = a_i$. For a matrix $\mathbf{A}$, $\mathbf{A}^\top$ stands for its transpose and $\mathbf{A}^+$ for its Moore-Penrose pseudo-inverse. Its maximum and minimum singular values are obtained as $\sigma_{\max}(\mathbf{A})$ and $\sigma_{\min}(\mathbf{A})$, and its spectral radius (i.e., the largest modulus of its eigenvalues) as $\rho(\mathbf{A})$. When it is symmetric, its maximum and minimum eigenvalue are denoted as $\lambda_{\max}(\mathbf{A})$ and $\lambda_{\min}(\mathbf{A})$, and its condition number is defined as $\kappa(\mathbf{A}) \triangleq {\lambda_{\max}(\mathbf{A})}/{\lambda_{\min}(\mathbf{A})}$. Given two matrices of same dimensions, $>$, $\geq$, $\leq$ and $<$ are element-wise inequalities. The sets of real scalars, size-n vectors and size-$m \times n$ matrices are denoted as $\mathbb{R}$, $\mathbb{R}^n$ and $\mathbb{R}^{m\times n}$, while $\mathcal{A} = [l; u]$ is the closed real interval between l and u. Given two sets $\mathcal{A}_1$ and $\mathcal{A}_2$, $\mathcal{A}_1 \bigtimes \mathcal{A}_2$ stands for their Cartesian product, and $\bigtimes_{q=1}^{Q} \mathcal{A}_q \triangleq \mathcal{A}_1 \bigtimes \ldots \bigtimes \mathcal{A}_Q$. The cardinality of $\mathcal{A}$ is denoted as $|\mathcal{A}|$. The set $2^{\mathcal{A}}$ is the power set of $\mathcal{A}$, i.e., the set of all its subsets. Given a (possibly vector) function $\mathbf{f}(\mathbf{x})$, $[\mathbf{f}(\mathbf{x})]_{\mathbf{a}}$ is another notation for $\mathbf{f}(\mathbf{a})$. For the scalar function $f(\mathbf{x}, \mathbf{y})$ with $\mathbf{x} \in \mathbb{R}^n$, $\mathbf{y} \in \mathbb{R}^m$, the vectors and matrices $\boldsymbol{\nabla}_{\mathbf{x}} f(\overline{\mathbf{x}}, \overline{\mathbf{y}}) \in \mathbb{R}^n$, $\boldsymbol{\nabla}^2_{\mathbf{xx}} f(\overline{\mathbf{x}}, \overline{\mathbf{y}}) \in \mathbb{R}^{n\times n}$ and $\boldsymbol{\nabla}^2_{\mathbf{xy}} f(\overline{\mathbf{x}}, \overline{\mathbf{y}}) \in \mathbb{R}^{n\times m}$ group the first and second-order derivatives evaluated at $(\overline{\mathbf{x}}, \overline{\mathbf{y}})$. When it is clear from the context, the distinction between the differentiation variables and the evaluation variables is not made. The gradient of a vector function $\mathbf{f}\colon \mathbb{R}^n \to \mathbb{R}^p$, evaluated at $\overline{\mathbf{x}}$ is denoted as $\boldsymbol{\nabla}_{\mathbf{x}} \mathbf{f}(\overline{\mathbf{x}}) \in \mathbb{R}^{p\times n}$. Finally, $\mathbb{P}[\alpha]$ is the probability for the event α to occur.

II. Random Access for Federated Learning

In order to introduce the class of problems which are tackled in this paper, an FL scenario is described in Section II-A, and the associated RA communication problem is presented in Section II-B.

A. Federated learning description

In an FL setting, a dataset, i.e. a collection of input/output pairs, is distributed among an ensemble of Q nodes. The aim of the nodes is to collectively infer a unique global model of the input/output relationship, valid across the whole distributed dataset. As represented in Figure 1, an FL algorithm achieves this by iteratively updating local and global versions of the model. More precisely, the learning process consists of K three-step rounds [5], named communication rounds in the literature, coordinated by a server collocated with an access point. These three steps are respectively the model

© 2024 IEEE. Personal use is permitted, but republication/redistribution requires IEEE permission. See https://www.ieee.org/publications/rights/index.html for more information.

This article has been accepted for publication in IEEE Internet of Things Journal. This is the author's version which has not been fully edited and content may change prior to final publication. Citation information: DOI 10.1109/JIOT.2024.3364756

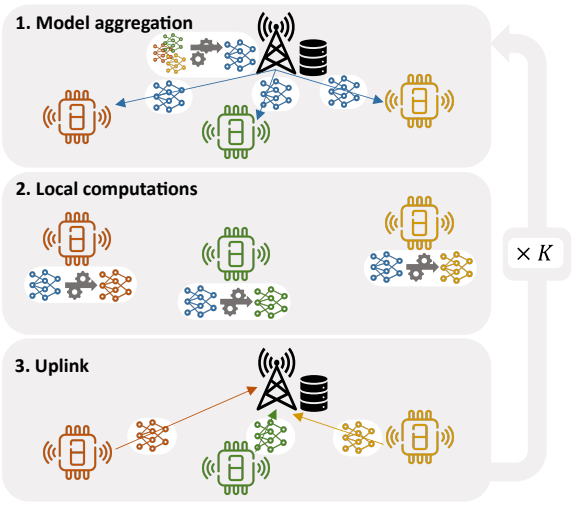


Fig. 1. FL protocol illustration, adapted from [7]. A server, collocated with an access point, implements a FL procedure with 3 workers. This procedure consists in K communication rounds of three steps each. The operations performed at each step are described in the white rectangles, the blue color refers to the access point, while the colors red, green and yellow correspond respectively to the first, second and third worker.

aggregation step, the local computation step, and the uplink communication step. During the aggregation step, the server fusions the previously received local models into a global model, and wirelessly sends it to the workers. Then, for the computation step, each qth worker performs τ_q local model updates. Finally, the updated models are communicated back to the server within the uplink communication step. As the workers may have different dataset sizes, computation and communication resources, FL algorithms may be improved by letting the server select only a subset $\mathcal{P}_k$ of the Q workers at each kth round [51], different at each communication round k. In such setting, workers with lower computation and communication durations will typically be selected more often than the others. At the condition that the subsets $\mathcal{P}_k$'s eventually span all Q workers, such mechanism enables to speed up the learning process. Assuming constant latencies across the communication rounds, the total learning time T_{tot} is thus obtained as

$$T_{\text{tot}} = \sum_{k=1}^{K} \left(T_0 + \max_{q \in \mathcal{P}_k} \{ \tau_q T_{\text{comp},q} + T_{\text{comm},q} \} \right), \tag{1}$$

with T_0 the aggregation step duration, $T_{\text{comp},q}$ the duration of one iteration of the local model update of the qth node, and $T_{\text{comm},q}$ the uplink communication duration for the qth node. While the local model updates are performed in parallel, the uplink step requires all workers to communicate with the unique access point, the total communication load scaling thus linearly with the number of workers. Hence, when there are many workers, this step becomes the bottleneck, and the multiple access scheme must thus be optimised. To keep the learning duration below a desired latency T_g, the access scheme must give to the qth node, when selected by the server, a rate greater than a minimum rate requirement $R_{\text{up},q}$. This minimum rate reads as

$$R_{\text{up},q} \triangleq \frac{s}{\frac{T_g}{K} - T_0 - \tau_q T_{\text{comp},q}}, \tag{2}$$

with s the model size. The numbers of local model updates τ_q and communication rounds K can be linked to the desired accuracy losses ϵ_l and ϵ_g, respectively at the end of the local model updates, and at the end of the global learning process. To remain general, these links are modelled with functions $\{f_q\}_{q=1}^{Q}$ and g, respectively giving the minimum number of local iterations and communication rounds required to reach the accuracy losses ϵ_l and ϵ_g:

$$\tau_q \geq f_q(\epsilon_l), \qquad K \geq g(\epsilon_l, \epsilon_g). \tag{3}$$

These function are such that the f_q's decrease with ϵ_l, while g increases with ϵ_l but decreases with ϵ_g [7], [11], [12], [52]. This work accommodates any model for τ_q and K, even experimental data which would provide the above relationships. It can also be noticed that the model f_q may be different for each worker. This enables to encompass FL protocols letting each worker decides how to achieved the desired local accuracy. To highlight the impact of the global parameters ϵ_g and T_g on the minimum rate requirement $R_{\text{up},q}$, this latter can be written as $R_{\text{up},q}(\epsilon_g, T_g)$ in the following, and it is represented in Figure 2.

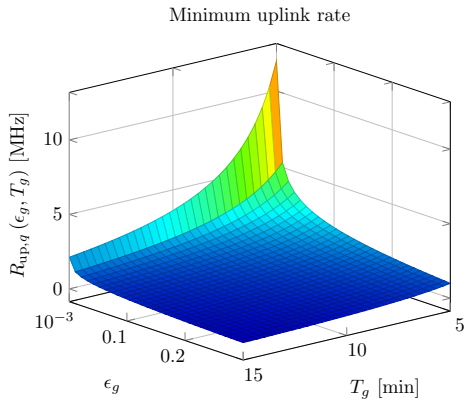


Fig. 2. Minimum uplink rate as a function of the global accuracy loss ϵ_g and learning duration T_g, from computation model and parameters of [7]. The model reads as $f_q(\epsilon_l) \triangleq C_1 \ln \frac{1}{\epsilon_l}$ whatever q and $g(\epsilon_l, \epsilon_g) = \frac{C_2}{1-\epsilon_l} \ln \frac{1}{\epsilon_g}$, and the parameters are $C_1 = 100.5$, $C_2 = 20$, $\epsilon_l = 0.1$, $T_0 = 0.33\,\text{s}$, $T_{\text{comp},q} = 3.3\,\text{ms}$ and $s = 10\,\text{Mb}$.

In order for the workers to have the knowledge of the minimum rate requirement (2), they must be aware of the accuracy models (3), and they must know the parameters s, T_g, ϵ_g, ϵ_l, T_0 and $T_{\text{comp},q}$. The quantities s, T_g, ϵ_g and ϵ_l will typically be specified by the application requiring the federated learning service. The durations T_0 and $T_{\text{comp},q}$, however, depend on the server and workers computation speed. They can be estimated from their hardware specifications, and on the information collected along their past operations.

B. Multiple access uplink communication scheme

The multiple access scheme must now be designed so as to support the minimum rate requirement of the many workers.

© 2024 IEEE. Personal use is permitted, but republication/redistribution requires IEEE permission. See https://www.ieee.org/publications/rights/index.html for more information.

This article has been accepted for publication in IEEE Internet of Things Journal. This is the author's version which has not been fully edited and content may change prior to final publication. Citation information: DOI 10.1109/JIOT.2024.3364756

To that aim, a slotted RA scheme is considered: common time slots are shared by the workers, which have some probability, named the access probability, to try to transmit part of the model to the access point on a given time slot. This probability must be carefully designed, as if several workers are active at the same time slots, then all communications are lost. As discussed in the introduction and in the literature, RA protocols are particularly suited to the uplink communication step of FL [28], [32], as they mitigate the signalling overhead. Also, the access probabilities of the devices can be seamlessly adapted to their heterogeneity: if one device suffers from poor propagation conditions, and thus from a low rate per communication slot, its access probability can be increased. This enables to increase the number of communication slots during which the device is active, and thus at the end to enable to support the transmission of the model. Moreover, since resources are not allocated device by device, RA schemes seamlessly adapt to the set of selected devices, which changes at each communication round. Furthermore, by giving the communication decisions to the workers, RA protocols scale very well with the number of devices. The drawback of these advantages is that a loss of performance with respect to orthogonal multiple access schemes is expected. The analysis carried out in this paper precisely enables to balance the above advantages with this performance loss, depending on the considered scenario.

The considered RA scheme is a slotted multi-level ALOHA-like protocol. As for the traditional ALOHA protocol, the uplink communication step is divided in N_s time slots, devices having some probability to send part of the updated model to the access point at each slot. The difference with respect to the traditional protocol, in which workers have one idle and one active level, lies in the fact that each qth worker has $A_q + 1$ levels, the 0th one being the idle state while the A_q others differ in terms of power and rate. The rate and communication power of the a_qth activity level are respectively denoted as R_{q,a_q} and P_{q,a_q}, with the idle state being such that $(R_{q,0}, P_{q,0}) = (0, 0)$. At each time slot, devices draw thus one of their state according to a probability profile $\mathbf{x}_q = \left[x_{q,a_q}\right]_{a_q=0}^{A_q}$ on its activity levels. With these elements, the FL scheme considered in this work is described by Algorithm 1, algorithm details being discussed below. In Algorithm 1, the notation $\cdot^{(k)}$ applies to all quantities which vary with the communication round, and denotes the quantity at communication round k. The global model which is broadcasted by the server at round k is denoted as $w^{(k)}$, while the model which has been updated by the qth worker is written as $w_q^{(k)}$. Finally, the notation $\tilde{w}_q^{(k)} \triangleq \left[w_q^{(k)}, x_{q,0}^{(k)}\right]$ denotes the updated model concatenated with the idle probability of the qth worker.

At each communication round, Algorithm 1 lets each selected worker design its probability profile, as described below by (6). Such choice depends on the worker interests, but must in all cases support the uplink communication of the FL task. In other words, the qth node, when selected by the server, must have an average rate higher than $R_{\text{up},q}$. This average rate depends both on the probability profile of the considered worker $\mathbf{x}_q$, and on the ones of all the other workers $\mathbf{x}_{-q} \triangleq [\mathbf{x}_r]_{r \neq q}$. It is computed as

$$\overline{R}_q\left(\mathbf{x}_q, \mathbf{x}_{-q}\right) \triangleq \sum_{a_q=1}^{A_q} x_{q,a_q} R_{q,a_q} \theta_{q,a_q}\left(\mathbf{x}_{-q}\right), \tag{4}$$

with $\theta_{q,a_q}\left(\mathbf{x}_{-q}\right)$ the communication success probability of the qth device when it employs activity level a_q. For a communication to be successful, no other selected worker should use the channel simultaneously, and the channel should support the targeted rate. Considering that for each communication round, each rth worker is selected independently with a probability $\mathbb{P}_r$ by the server[1], the probability that the rth worker transmits during one slot is given by $\left(1 - x_{r,0}\right)\mathbb{P}_r$. Thus, $\theta_{q,a_q}\left(\mathbf{x}_{-q}\right)$ reads as

$$\theta_{q,a_q}\left(\mathbf{x}_{-q}\right) \triangleq \mathbb{P}_{\text{cov},a_q,q} \prod_{r \neq q} \left(1 - \mathbb{P}_r + \mathbb{P}_r x_{r,0}\right), \tag{5}$$

with $\mathbb{P}_{\text{cov},a_q,q}$ the probability the targeted rate is below the channel capacity, named the coverage probability. It depends on the fading statistics, and can be computed as $\mathbb{P}_{\text{cov},a_q,q} \triangleq \mathbb{P}\left[B \log_2\left(1 + \frac{P_{q,a_q}|h_q|^2}{\gamma_n B}\right) \geq R_{q,a_q}\right]$, with B the bandwidth, $|h_q|^2 \triangleq L_q \zeta_q$ the channel power gain including the path loss L_q and the small-scale fading ζ_q, and γ_n the noise power spectral density. This coverage probability can be obtained from the Cumulative Distribution Function (CDF) of ζ_q, written $F_{\zeta_q}(x)$, as

$$\mathbb{P}_{\text{cov},a_q,q} = 1 - F_{\zeta_q}\left(\frac{\gamma_n B\left(2^{\frac{R_{q,a_q}}{B}} - 1\right)}{P_{q,a_q} L_q}\right).$$

It should be noted that the other workers' impact lies in the $\left(1 - \mathbb{P}_r + \mathbb{P}_r x_{r,0}\right)$ factors of the success probability expression (5). Indeed, these factors are between 0 and 1, and thus they decrease the success probability as the number of workers

Algorithm 1 FL with uplink RA optimisation - qth node

Select an initial probability profile $\mathbf{x}_q^{(0)}$ with $x_{q,0}^{(0)} \geq 1 - x_q^{\max}$
for $k = 1, \ldots, K$ **do**
  if Selected at round k **then**
    Receive the global model $w^{(k)}$
    Receive $X^{(k)} \triangleq \prod_{q=1}^{Q} 1 - \mathbb{P}_q + \mathbb{P}_q x_{q,0}^{(k-1)}$
    Compute $\theta_{q,a_q}\left(\mathbf{x}_{-q}\right) = \mathbb{P}_{\text{cov},a_q,q} \frac{X^{(k)}}{1 - \mathbb{P}_q + \mathbb{P}_q x_{q,0}^{(k-1)}}$
    Obtain the updated model $w_q^{(k)}$ after τ_q local updates
    Design the probability profile $\mathbf{x}_q^{(k)}$ according to (6)
    Let $\tilde{w}_q^{(k)} \triangleq \left[w_q^{(k)}, x_{q,0}^{(k)}\right]$
    for $n = 1, \ldots, N_s$ **do**
      Draw a_q according to $\mathbf{x}_q^{(k)}$
      Using activity level a_q, send part of $\tilde{w}_q^{(k)}$

[1]As explained above, the worker selection might depend on their computation and communication resources. By adapting the selection probability to the workers capability, the system model considered in this paper enables to mimic selection schemes such as the one of [51].

© 2024 IEEE. Personal use is permitted, but republication/redistribution requires IEEE permission. See https://www.ieee.org/publications/rights/index.html for more information.

This article has been accepted for publication in IEEE Internet of Things Journal. This is the author's version which has not been fully edited and content may change prior to final publication. Citation information: DOI 10.1109/JIOT.2024.3364756

increases. Additionally to the rate constraint, a maximum active probability $x_q^{\max}$ is considered to avoid channel congestion. This maximum active probability depicts the sharing of the communication resource among the workers, and thus scales as $\mathcal{O}\left(\frac{1}{Q}\right)$. A method to select an adequate value for this parameter as a function of the FL parameters is moreover discussed in Section V. To conclude the devices' description, each one is associated with an utopia probability profile $\mathbf{x}_q^{(u)}$, being its ideal utilisation profile. Such profile models his interest, which can depend on the consumed energy, monetary incentives involved in the FL process, type of the devices, etc. An utopia profile example is given in Section V-B, for workers minimising their power consumption.

With these elements, the probability profile design of the qth device is captured by the following optimisation problem,

$$\begin{array}{ll} \min_{\mathbf{x}_q} & \left\|\mathbf{x}_q - \mathbf{x}_q^{(u)}\right\|_2^2, \\ \text{s.t.} & 1 - x_q^{\max} \leq x_{q,0}, \\ & 0 \leq x_{q,a_q}, \quad \forall a_q = 1, \ldots, A_q, \\ & \sum_{a_q=0}^{A_q} x_{q,a_q} = 1, \\ & \overline{R}_q\left(x_q, \mathbf{x}_{-q}\right) \geq R_{\text{up},q}. \end{array} \tag{6}$$

This optimisation problem is a quadratic program, which can efficiently be solved using specialised solvers, or with the Dijkstra alternating projection method [53]. To that aim, the qth node must know at each communication round the success probability of all its activity levels. This can be achieved in the following manner. Each qth node appends a header containing $x_{q,0}$ to the model during the uplink communication. Then, the server computes the value $X \triangleq \prod_{q=1}^{Q}\left(1 - \mathbb{P}_q + \mathbb{P}_q x_{q,0}\right)$, either based on the received probabilities, or based on probabilities of the previous round for inactive nodes. Next, X is sent together with the model during the downlink communication step. Each node can finally compute the success probability of its a_qth activity level as $\theta_{q,a_q}\left(\mathbf{x}_{-q}\right) = \mathbb{P}_{\text{cov},a_q,q}\frac{X}{1-\mathbb{P}_q+\mathbb{P}_q x_{q,0}}$. By transmitting the product X instead of all $x_{q,0}$'s, the header sizes are constant whatever the number of nodes Q, and insignificant with respect to the model size s.

The challenge raised by the above is that the optimisation problems of the Q nodes are coupled together through their rate constraint. Thus, the optimum probability profile of each node, named the Best Response (BR), changes at each communication round depending on the probability profile of the other nodes. Moreover, such changes are asynchronous since in Algorithm 1, only the devices selected by the server are allowed to modify and communicate back their probability profile. Ensuring the asynchronous BR updates quickly reach an equilibrium at which the FL task runs smoothly is therefore critical. Such updates are named in the literature the asynchronous BRD, while the problem of getting an equilibrium of optimisation problems coupled through their constraints is an instance of a GNEP. However, the literature does not provide convergence guarantees for the BRD of a GNEP, especially as the considered GNEP is neither jointly convex, nor a generalised potential game. Hence, the aim of this paper is precisely to develop such a framework. This will enable to get insights on the levers the server has to control the interactions, and in particular on the maximum active probabilities $x_q^{\max}$ and on the available activity levels. Below, a general framework able to analyse the BRD of GNEPs is first developed in Section III and Section IV, and then applied to the FL setting in Section V.

III. GNEP Class Definition

In the above section, an FL scenario has been considered, in which devices must adapt their activity profile based on the ones of the others. Their interaction comes from their coupled rate constraints, which make such problem an instance of a GNEP. In this section, the formal definition of a GNEP is first provided in Section III-A, and then the class of GNEPs considered in this work is delimited in Section III-B. Finally, the BRD definition is introduced in Section III-C. These definitions will enable to provide BRD convergence conditions in the next section.

A. Generalised Nash Equilibrium Problem Definition

A GNEP models the interactions between Q players indexed in $\Omega = \{1, \ldots, Q\}$, each controlling a n_q-dimensional vector of variables, denoted $\mathbf{x}_q$ and named its strategy. The strategy profile of all players can either be denoted as $\overline{\mathbf{x}}$ or $(\mathbf{x}_q, \mathbf{x}_{-q})$, with $\mathbf{x}_{-q} \triangleq \{\mathbf{x}_q\}_{r \neq q}$ denoting the strategy profile of all players except the q-th one. For each q-th player, the fixed set $\overline{\mathcal{X}}_q$, and the player-dependent strategy set $\mathcal{X}_q\left(\mathbf{x}_{-q}\right) : \overline{\mathcal{X}}_{-q} \to 2^{\overline{\mathcal{X}}_q}$ are introduced, with $\overline{\mathcal{X}}_{-q} \triangleq \bigtimes_{r \neq q} \overline{\mathcal{X}}_q$. The notation $2^{\overline{\mathcal{X}}_q}$ denotes the power set of $\overline{\mathcal{X}}_q$, i.e., the set of all its subsets. The above strategy set definition implies thus that $\mathcal{X}_q\left(\mathbf{x}_{-q}\right) \subseteq \overline{\mathcal{X}}_q$, whatever $\mathbf{x}_{-q} \in \overline{\mathcal{X}}_{-q}$. Thus, the sets $\overline{\mathcal{X}}_q$ delimit the extreme-values of the strategy-dependent sets. Letting $\overline{\mathcal{X}} \triangleq \bigtimes_{q=1}^{Q} \overline{\mathcal{X}}_q$, the set $\mathcal{Y}_q$ is furthermore introduced as $\mathcal{Y}_q \triangleq \left\{\overline{\mathbf{x}} \middle| \mathbf{x}_{-q} \in \overline{\mathcal{X}}_q, \mathbf{x}_q \in \mathcal{X}_q\left(\mathbf{x}_{-q}\right)\right\}$, representing the global strategy profile which are feasible for the q-th player given $\mathbf{x}_{-q}$. Constrained by its player-dependent strategy set, the q-th player targets the minimisation of the objective function $u_q\left(\mathbf{x}_q, \mathbf{x}_{-q}\right) : \mathcal{Y}_q \to \mathbb{R}$. The players' interaction reads thus as

$$\begin{array}{ll} \text{minimise}_{\mathbf{x}_q} & u_q\left(\mathbf{x}_q, \mathbf{x}_{-q}\right), \\ \text{s.t.} & \mathbf{x}_q \in \mathcal{X}_q\left(\mathbf{x}_{-q}\right). \end{array} \tag{7}$$

Given a strategy profile of the other players $\mathbf{x}_{-q}$, the minimisers of the above problem are grouped into the set $\mathcal{BR}_q\left(\mathbf{x}_{-q}\right)$, named the BR set. In this context, an equilibrium $\mathbf{x}^E \in \overline{\mathcal{X}}$ of a GNEP is such that $\mathbf{x}_q^E \in \mathcal{BR}_q\left(\mathbf{x}_{-q}^E\right)\ \forall q \in \Omega$, i.e. they are the fixed points of the BR mapping.

B. Considered GNEP class

The GNEPs tackled in this work are limited to the class which we named *GNEPs with polyhedral strategy sets and variable right-hand sides*. GNEPs belonging to this class are those whose set-valued mappings $\mathcal{X}_q\left(\mathbf{x}_{-q}\right)$ can be written as

$$\mathcal{X}_q\left(\mathbf{x}_{-q}\right) = \left\{\mathbf{x}_q \in \mathbb{R}^{n_q} \middle| \begin{array}{ll} \mathbf{p}_{q,i}^\top \mathbf{x}_q \leq \gamma_{q,i}\left(\mathbf{x}_{-q}\right), & \forall i \in \mathcal{I}_q \\ \tilde{\mathbf{p}}_{q,j}^\top \mathbf{x}_q = \tilde{\gamma}_{q,j}\left(\mathbf{x}_{-q}\right), & \forall j \in \mathcal{J}_q \end{array}\right\}, \tag{8}$$

with $\mathcal{I}_q \triangleq \{1, \ldots, I_q\}$ and $\mathcal{J}_q \triangleq \{1, \ldots, J_q\}$ the sets of inequality and equality constraints, and $\gamma_{q,i} \colon \overline{\mathcal{X}}_{-q} \to \mathbb{R}$,

© 2024 IEEE. Personal use is permitted, but republication/redistribution requires IEEE permission. See https://www.ieee.org/publications/rights/index.html for more information.

This article has been accepted for publication in IEEE Internet of Things Journal. This is the author's version which has not been fully edited and content may change prior to final publication. Citation information: DOI 10.1109/JIOT.2024.3364756

$\tilde{\gamma}_{q,j}\colon \overline{\mathcal{X}}_{-q} \to \mathbb{R}$ the possibly non-linear Right-Hand Side (RHS) functions which depend on the other players. The sets $\mathcal{I}^{\circ}_{qr} \subseteq \mathcal{I}_q$ and $\mathcal{J}^{\circ}_{qr} \subseteq \mathcal{J}_q$ are furthermore introduced as the sets of constraints for which the RHS function depends on the strategy of the r-th player. The GNEPs are furthermore assumed to satisfy the four below assumptions, the first three being standard in the GNEP literature. In Assumption 2, $\mathcal{C}^k$ is the class of functions which are continuously differentiable up to the kth order.

Assumption 1 (Convexity and non-emptiness)**.** *For each q-th player, $\forall \mathbf{x}_{-q} \in \overline{\mathcal{X}}_q$,*

- *$\mathcal{X}_q(\mathbf{x}_{-q})$ is non-empty and bounded;*
- *$\overline{\mathcal{X}}_q$ is compact and convex;*
- *$u_q(\mathbf{x}_q, \mathbf{x}_{-q})$ is strongly convex in $\mathbf{x}_q$ on $\mathcal{X}_q(\mathbf{x}_{-q})$.*

Assumption 2 (Continuity and differentiability)**.** *For each q-th player, $\forall \overline{\mathbf{x}} \in \mathcal{Y}_q$,*

- *$u_q(\mathbf{x}_q, \mathbf{x}_{-q})$ is $\mathcal{C}^2$ in $\mathbf{x}_q$;*
- *$\boldsymbol{\nabla}_{\mathbf{x}_q} u_q(\mathbf{x}_q, \mathbf{x}_{-q})$ is $\mathcal{C}^1$ in $\mathbf{x}_{-q}$;*
- *$\{\gamma_{q,i}(\mathbf{x}_{-q})\}_{i\in\mathcal{I}_q}$ and $\{\tilde{\gamma}_{q,j}(\mathbf{x}_{-q})\}_{j\in\mathcal{J}_q}$ are $\mathcal{C}^1$ in $\mathbf{x}_{-q}$.*

Assumption 3 (Constraint qualification)**.** *For each q-th player,*

- *$\forall \mathbf{x}_{-q} \in \overline{\mathcal{X}}_{-q}$, the Slater constraint qualification holds for $\mathcal{X}_q(\mathbf{x}_{-q})$, i.e., $\exists \mathbf{x}_q \in \mathcal{X}_q(\mathbf{x}_{-q})$ such that $\forall i \in \mathcal{I}_q$, $\mathbf{p}_{q,i}^{\top}\mathbf{x}_q < \gamma_{q,i}(\mathbf{x}_{-q})$.*
- *The family $\{\tilde{\mathbf{p}}_{q,j}\}_{j\in\mathcal{J}_q}$ is linearly independent.*

Assumption 1 ensures that the optimisation problem of the q-th player always admits a unique solution. In that case, the BR mapping of the q-th player is single-valued and denoted as $\mathbf{BR}_q(\mathbf{x}_{-q})\colon \overline{\mathcal{X}}_{-q} \to \overline{\mathcal{X}}_q$. The GNEP equilibria are then points $\mathbf{x}^E \in \overline{\mathcal{X}}$ such that $\mathbf{x}^E_q = \mathbf{BR}_q(\mathbf{x}^E_{-q})\ \forall q \in \Omega$. Grouping the BR mapping of all players, the global BR mapping is defined as $\mathbf{BR}(\overline{\mathbf{x}}) \triangleq \{\mathbf{BR}_q(\mathbf{x}_{-q})\}_{q=1}^{Q}\colon \overline{\mathcal{X}} \to \overline{\mathcal{X}}$, and equilibrium points are equivalently defined as points satisfying $\mathbf{x}^E = \mathbf{BR}(\mathbf{x}^E)$.

To state the last assumption, given $\overline{\mathbf{x}}$, the set of active inequality constraints is defined as

$$\mathcal{I}^{\overline{\mathbf{x}}}_q \triangleq \left\{ i \in \mathcal{I}_q \middle| \mathbf{p}_{q,i}^{\top}\mathbf{x}_q = \gamma_{q,i}(\mathbf{x}_{-q}) \right\}. \tag{9}$$

Then, the ensemble of all sets of linearly independent constraints which can be active at the same time, with at least one depending on the r-th player is introduced as

$$\mathfrak{I}^{\dagger}_{qr} \triangleq \left\{ \mathcal{I} \subseteq \mathcal{I}_q \middle| \begin{array}{l} \exists \overline{\mathbf{x}} \in \mathcal{Y}_q \text{ s.t. } \mathcal{I} = \mathcal{I}^{\overline{\mathbf{x}}}_q \\ \left\{\{\mathbf{p}_i\}_{i\in\mathcal{I}}, \{\tilde{\mathbf{p}}_j\}_{j\in\mathcal{J}}\right\} \text{ is lin. indep.} \\ \mathcal{I} \cap \mathcal{I}^{\circ}_{qr} \neq \emptyset \text{ or } \mathcal{J} \cap \mathcal{J}^{\circ}_{qr} \neq \emptyset \end{array} \right\}, \tag{10}$$

where lin. indep. abbreviates linearly independent. The problem is also looked at when the inequality constraints are perturbed by $\mathbf{v}_q \in \mathbb{R}^{I_q}$, and the following sets are defined similarly to the above:

$$\mathcal{K}^{\overline{\mathbf{x}},\mathbf{v}_q}_q \triangleq \left\{ i \in \mathcal{I}_q \middle| \mathbf{p}_{q,i}^{\top}\mathbf{x}_q = \gamma_{q,i}(\mathbf{x}_{-q}) + v_{q,i} \right\}, \tag{11}$$

$$\mathfrak{K}^{\dagger}_{qr} \triangleq \left\{ \mathcal{I} \subseteq \mathcal{I}_q \middle| \begin{array}{l} \forall \epsilon > 0, \exists \overline{\mathbf{x}} \in \mathcal{Y}_q, \mathbf{v}_q \in \mathbb{R}^{I_q} \\ \quad \text{with } \|\mathbf{v}_q\|_2 \leq \epsilon \text{ s.t. } \mathcal{I} = \mathcal{K}^{\overline{\mathbf{x}},\mathbf{v}_q}_q \\ \left\{\{\mathbf{p}_i\}_{i\in\mathcal{I}}, \{\tilde{\mathbf{p}}_j\}_{j\in\mathcal{J}}\right\} \text{ is lin. indep.} \\ \mathcal{I} \cap \mathcal{I}^{\circ}_{qr} \neq \emptyset \text{ or } \mathcal{J} \cap \mathcal{J}^{\circ}_{qr} \neq \emptyset \end{array} \right\}. \tag{12}$$

Assumption 4 (Set insensitivity to perturbations)**.** *For each pair (q, r) of players, with $q \neq r$, $\mathfrak{K}^{\dagger}_{qr} = \mathfrak{I}^{\dagger}_{qr}$.*

The above assumption means that when considering infinitesimally small perturbations, the sets of possibly active constraints are not modified. To better grasp this last assumption, the below example illustrates its impact.

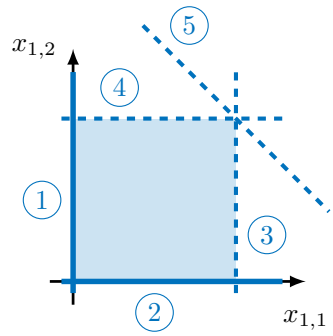


Fig. 3. Strategy set of Example 1, the constraint index being denoted by circled numbers. The moving constraints are depicted with dashed lines.

Example 1. *Let us consider a two-player GNEP, in which the first player controls a size-2 vector $\mathbf{x}_1 \triangleq [x_{1,1}, x_{1,2}]^{\top}$ and the second a scalar strategy $x_2 \in \overline{\mathcal{X}}_2 = [0\,;\,1]$. The strategy set of the first reads as*

$$\mathcal{X}_1(x_2) \triangleq \left\{ \mathbf{x}_1 \in \mathbb{R}^2 \middle| \begin{array}{l} [-1 \quad 0]\,\mathbf{x}_1 \leq 0 \\ [0 \quad -1]\,\mathbf{x}_1 \leq 0 \\ [1 \quad 0]\,\mathbf{x}_1 \leq x_2 \\ [0 \quad 1]\,\mathbf{x}_1 \leq x_2 \\ [1 \quad 1]\,\mathbf{x}_1 \leq 2x_2 \end{array} \right\},$$

being represented in Figure 3. Constraint 5 can be seen to be redundant with the others. As constraints 3, 4 and 5 depends on the second player, this gives $\mathcal{I}^{\circ}_{12} = \{3, 4, 5\}$. Depending on $\overline{\mathbf{x}}$, the set $\mathcal{I}^{\overline{\mathbf{x}}}_q \in \{\emptyset, \{1\}, \{1, 2\}, \{2\}, \{2, 3\}, \{3\}, \{3, 4, 5\}, \{4\}, \{4, 1\}\}$. Removing the linearly dependent constraints, and the sets which do not depend on the second player, $\mathfrak{I}^{\dagger}_{12} = \{\{2, 3\}, \{3\}, \{4\}, \{4, 1\}\}$. Yet, considering infinitesimal perturbations of constraints 3, 4 and 5, $\mathcal{K}^{\overline{\mathbf{x}},\mathbf{v}}_q \in \{\emptyset, \{1\}, \{1, 2\}, \{2\}, \{2, 3\}, \{3\}, \{3, 4, 5\}, \{4\}, \{4, 1\}\} \cup \{\{3, 4\}, \{4, 5\}, \{3, 5\}\}$. This gives $\mathfrak{K}^{\dagger}_{12} = \{\{2, 3\}, \{3\}, \{4\}, \{4, 1\}\} \cup \{\{3, 4\}, \{4, 5\}, \{3, 5\}\}$, which is different from $\mathfrak{I}^{\dagger}_{12}$. This is an example of a pathological case in which the constraint sets are sensitive to infinitesimally small perturbations, and which are thus not covered by this paper. As it can be noticed, this happens because the fifth constraint follows the third and fourth one whatever x_2, and therefore is redundant. If one considers the same problem but with the fifth constraint removed, then this equivalent formulation becomes insensitive to perturbations.

© 2024 IEEE. Personal use is permitted, but republication/redistribution requires IEEE permission. See https://www.ieee.org/publications/rights/index.html for more information.

This article has been accepted for publication in IEEE Internet of Things Journal. This is the author's version which has not been fully edited and content may change prior to final publication. Citation information: DOI 10.1109/JIOT.2024.3364756

C. Best response dynamics definition

As detailed above, this work considers the dynamics naturally arising from a GNEP: the BRD. Such dynamics lets players iteratively update their strategy according to their BR, and it can respectively be termed synchronous, sequential or totally asynchronous if all players update their strategy respectively at the same time, one after the other or at any desired time, with possibly outdated information on the other players strategy.

For the sake of the BRD definition, each q-th player is associated with a set $\mathcal{N}_q$ of its update times and with the times $\left\{\left\{\tau_r^q(n)\right\}_{r\neq q}\right\}_{n\in\mathcal{N}_q}$ which denote the fact that at time n, the q-th player knows the strategy of the r-th player which has been used at time $\tau_r^q(n)$, and not the current one. Naturally, these times are such that $\tau_r^q(n) \leq n$, as players can only use past and current information. Let $\mathbf{x}_q^{(n)}$ be the strategy of the q-th player at time n, and define the strategy profile of other players as seen at time n by the q-th player as $\mathbf{x}_{-q}^{(\boldsymbol{\tau}^q(n))} = \left\{\mathbf{x}_r^{(\tau_r^q(n))}\right\}_{r\neq q}$. With these definitions, the BRD is described by Algorithm 2

Algorithm 2 Totally Asynchronous Best Response Dynamics

Set $\mathbf{x}^{(0)} \in \overline{\mathcal{X}}$.
for $n = 0 \to \infty$ **do**
  for $q = 1, \ldots, Q$ **do**

$$\mathbf{x}_q^{(n+1)} = \begin{cases} \mathbf{BR}_q\left(\mathbf{x}_{-q}^{(\boldsymbol{\tau}^q(n))}\right) & \text{if } n \in \mathcal{N}_q, \\ \mathbf{x}_q^{(n)} & \text{otherwise.} \end{cases}$$

The synchronous (resp. sequential) BRD is obtained by setting the qth player update times as $\mathcal{N}_q = \{1, 2, \ldots\}$ (resp. $\mathcal{N}_q = \{q, q+Q, q+2Q, \ldots\}$), with up-to-date information: $\tau_r^q(n) = n$, $\forall n \in \mathcal{N}_q$, $\forall q, r \in \Omega$ with $q \neq r$. In the asynchronous case, for the BRD to be well-defined, the below assumption is introduced [54], naturally holding in any practical scenario.

Assumption 5 (BRD)**.** *For each q-th player,*

- *its strategy is updated infinitely often: $|\mathcal{N}_q| = \infty$;*
- *the outdated information about any r-th player is eventually purged from the system: $\lim_{k\to\infty} \tau_r^q(n_k) = \infty$ with $\{n_k\}$ an increasing sequence in $\mathcal{N}_q$.*

The first part of the assumption prevents some of the players from stopping the updates of their strategy, while the second ensures that as the time grows, they eventually base their updates on up-to-date information.

IV. Convergence of the Best Response Dynamics towards an Equilibrium

In this section, sufficient conditions ensuring the existence and unicity of an equilibrium, as well as the convergence of the BRD towards it, are obtained. These conditions, formally stated below in Theorem 1, are the major theoretical contribution of this paper. They depend on a convergence matrix $\boldsymbol{\Gamma} \in \mathbb{R}^{Q\times Q}$, which translates both the objective functions' interaction and the strategy sets' interaction. This matrix is obtained as

$$[\boldsymbol{\Gamma}]_{qr} \triangleq \sqrt{\left(\left[\boldsymbol{\Gamma}^{\text{obj}}\right]_{qr}\right)^2 + \left([\boldsymbol{\Gamma}^{\text{cons}}]_{qr}\right)^2}, \tag{13}$$

with $\boldsymbol{\Gamma}^{\text{obj}}, \boldsymbol{\Gamma}^{\text{cons}} \in \mathbb{R}^{Q\times Q}$. The objective part is computed as

$$\left[\boldsymbol{\Gamma}^{\text{obj}}\right]_{qr} \triangleq \begin{cases} \max_{\overline{\mathbf{x}}\in\overline{\mathcal{X}}} \frac{\sigma_{\max}\left(\boldsymbol{\nabla}^2_{\mathbf{x}_q\mathbf{x}_r} u_q(\overline{\mathbf{x}})\right)}{\lambda_{\min}\left(\boldsymbol{\nabla}^2_{\mathbf{x}_q\mathbf{x}_q} u_q(\overline{\mathbf{x}})\right)} & \text{if } q \neq r, \\ 0 & \text{otherwise.} \end{cases} \tag{14}$$

The constraint part is build as

$$[\boldsymbol{\Gamma}^{\text{cons}}]_{qr} \triangleq \begin{cases} C_{qr} & \text{if } q \neq r, \\ 0 & \text{otherwise,} \end{cases} \tag{15}$$

with, when $q \neq r$,

$$C_{qr} \triangleq \max_{\substack{\overline{\mathbf{x}}\in\overline{\mathcal{X}} \\ \mathcal{I}\in\mathfrak{I}_{qr}^\dagger}} \left\{\kappa\left(\boldsymbol{\nabla}^2_{\mathbf{x}_q\mathbf{x}_q} u_q(\overline{\mathbf{x}})\right) \sigma_{\max}\left(\left(\mathbf{E}_{qr,\mathcal{I}}\boldsymbol{\Pi}_{qr,\mathcal{I}}\right)^+ \mathbf{G}_{qr,\mathcal{I}}(\mathbf{x}_{-q})\right)\right\}, \tag{16}$$

where $\kappa(\cdot) \triangleq \frac{\lambda_{\max}(\cdot)}{\lambda_{\min}(\cdot)}$ is the condition number of a symmetric matrix and $(\cdot)^+$ the Moore-Penrose inverse operator. For each $\mathcal{I} \in \mathfrak{I}_{qr}^\dagger$, the above matrices are defined as

$$\mathbf{E}_{qr,\mathcal{I}} \triangleq \begin{bmatrix} \left\{\mathbf{p}_{q,i}^\top\right\}_{i\in\mathcal{I}_{qr}^{(e)}} \\ \left\{\tilde{\mathbf{p}}_{q,j}^\top\right\}_{j\in\mathcal{J}_{qr}^\circ} \end{bmatrix}, \qquad \mathbf{F}_{qr,\mathcal{I}} \triangleq \begin{bmatrix} \left\{\mathbf{p}_{q,i}^\top\right\}_{i\in\mathcal{I}_{qr}^{(f)}} \\ \left\{\tilde{\mathbf{p}}_{q,j}^\top\right\}_{j\in\mathcal{J}_q\setminus\mathcal{J}_{qr}^\circ} \end{bmatrix},$$

$$\boldsymbol{\Pi}_{qr,\mathcal{I}} \triangleq \mathbf{I} - \mathbf{F}_{qr,\mathcal{I}}^\top\left(\mathbf{F}_{qr,\mathcal{I}}\mathbf{F}_{qr,\mathcal{I}}^\top\right)^{-1}\mathbf{F}_{qr,\mathcal{I}},$$

$$\mathbf{G}_{qr,\mathcal{I}}(\mathbf{x}_{-q}) \triangleq \begin{bmatrix} \left\{\boldsymbol{\nabla}_{\mathbf{x}_r}^\top \gamma_{q,i}(\mathbf{x}_{-q})\right\}_{i\in\mathcal{I}_{qr}^{(e)}} \\ \left\{\boldsymbol{\nabla}_{\mathbf{x}_r}^\top \tilde{\gamma}_{q,j}(\mathbf{x}_{-q})\right\}_{j\in\mathcal{J}_{qr}^\circ} \end{bmatrix},$$

with the inequality constraint indices partitioned between $\mathcal{I}_{qr}^{(e)} \triangleq \mathcal{I} \cap \mathcal{I}_{qr}^\circ$, and $\mathcal{I}_{qr}^{(f)} \triangleq \mathcal{I} \setminus \mathcal{I}_{qr}^{(e)}$. The matrix $\boldsymbol{\Pi}_{qr,\mathcal{I}}$ is the projector onto the null space of $\mathbf{F}_{qr,\mathcal{I}}$, being well-defined since constraint sets of $\mathfrak{I}_{qr}^\dagger$ are linearly independent, ensuring $\mathbf{F}_{qr,\mathcal{I}}$ is full row rank. If $\mathbf{F}_{qr,\mathcal{I}}$ is empty, the above must be understood as $\boldsymbol{\Pi}_{qr,\mathcal{I}} = \mathbf{I}$. The definition of the convergence matrix $\boldsymbol{\Gamma}$ enables to state the main theorem of this paper, guaranteeing convergence of the BRD associated with a GNEP.

Theorem 1. *If a GNEP with polyhedral strategy sets and variable right-hand sides fulfils Assumptions 1 to 4 , and if it satisfies $\rho(\boldsymbol{\Gamma}) < 1$, then*

- *it admits a unique equilibrium $\mathbf{x}^E$;*
- *the totally asynchronous BRD, if it respects Assumption 5, converges to the equilibrium $\mathbf{x}^E$;*
- *the iterates $\mathbf{x}^{(n)}$ of the synchronous BRD converges linearly to $\mathbf{x}^E$ with a rate $\rho(\boldsymbol{\Gamma})$:*

$$\left\|\mathbf{x}^{(n)} - \mathbf{x}^E\right\| \leq C\left(\rho(\boldsymbol{\Gamma})\right)^n \left\|\mathbf{x}^{(0)} - \mathbf{x}^E\right\|,$$

C being a constant depending on the choice of norm.

Proof. The proof amounts at showing that the GNEP BR mapping $\mathbf{BR}(\overline{\mathbf{x}}) : \overline{\mathcal{X}} \to \overline{\mathcal{X}}$ is a contraction under some well-chosen block-maximum norm, $\overline{\mathcal{X}}$ being a compact set. Then,

© 2024 IEEE. Personal use is permitted, but republication/redistribution requires IEEE permission. See https://www.ieee.org/publications/rights/index.html for more information.

This article has been accepted for publication in IEEE Internet of Things Journal. This is the author's version which has not been fully edited and content may change prior to final publication. Citation information: DOI 10.1109/JIOT.2024.3364756

from [54, Chapter 3 and 6], the above theorem is obtained. The challenge lies in proving that $\rho(\mathbf{\Gamma}) < 1$ provides a sufficient condition for the contraction property of the BR mapping, as detailed in Appendix A. □

The above theorem provides a sufficient condition for the convergence of the BRD. What is particularly interesting with this theorem is that it describes a systematic procedure for any GNEP with polyhedral strategy sets and variable RHSs. This procedure consists in building the convergence matrices of the objective part and constraint part, and then computing the spectral radius of $\mathbf{\Gamma}$. Nevertheless, finding the maximum over all strategies $\overline{\mathbf{x}} \in \overline{\mathcal{X}}$ might be difficult for some problems, especially when there are many players and when the strategy sets are high-dimensional. In such cases, it must be kept in mind that any upper-bound for the off-diagonal elements can also be considered. This will lead to a convergence matrix $\tilde{\mathbf{\Gamma}}$ with a greater spectral radius [55, Fact 4.11.18], and thus $\rho\left(\tilde{\mathbf{\Gamma}}\right) < 1$ also provides existence and convergence guarantees.

To the authors' knowledge, the above theorem is the first result providing a framework able to study the convergence of the totally asynchronous BRD of a GNEP. Even for the peculiar class of generalised potential games, the convergence guarantees provided in [49] only hold if the BRD is regularised by some 2-norm objective function. If instead the classical Nash equilibrium problems are considered, i.e., those with fixed strategy sets, then the above theorem boils down to the state-of-the-art results of [3]. As far as the existence is concerned, it in fact holds under Assumptions 1 to 3 only, whatever the spectral radius value [4, Theorem 6]. A GNEP for which existence holds but not convergence is of little interest for an autonomous system. This is why the existence result is provided together with the convergence conditions in Theorem 1.

Before moving to the FL scenario analysis, a toy example is studied in order to illustrate the procedure provided by Theorem 1.

Example 2. *A two-player GNEP $\mathcal{G}^c$ parametrised by $0 < c < 1.5$ is considered. The players' objective functions and strategy sets are defined as*

$$\begin{cases} u_1(x_1, x_2) = (x_1 - cx_2 + 1)^2, \\ \mathcal{X}_1(x_2) = \overline{X}_1 = [-2; 2], \end{cases} \tag{17}$$

$$\begin{cases} u_2(x_2, x_1) = (x_2 + cx_1)^2, \\ \mathcal{X}_2(x_1) = \left[1 - cx_1; 3 - c\tfrac{x_1}{2}\right], \\ \overline{X}_2 = [1 - 2c; 3 + c]. \end{cases} \tag{18}$$

The first player is thus a classic player while the second is characteristic of GNEPs since his strategy set depends on x_1. The associated BR mappings are obtained by solving the quadratic univariate optimisation problems defined by (17) *and* (18)*. By inspection, the BRs are obtained as*

$$\begin{aligned} \mathrm{BR}_1(x_2) &= \min\{\max\{cx_2 - 1, -2\}, 2\}, \\ \mathrm{BR}_2(x_1) &= 1 - cx_1, \end{aligned}$$

as displayed in Figure 4. As it can be observed from the optimisation problems and strategy set mappings, or from the BR mappings, the parameter c measures in some sense the players' coupling. Players are independent when $c = 0$, slightly coupled for small c's while they become highly coupled as c increases. Analysing the fixed points of these BR mappings, it appears the GNEP has a unique equilibrium given by $\mathbf{x}^E = \left[\frac{c-1}{c^2+1}, \frac{c+1}{c^2+1}\right]$. The sequential BRD, obtained with $\mathcal{N}_1 = \{2, 4, 6, \ldots\}$ and $\mathcal{N}_2 = \{1, 3, 5, \ldots\}$, is depicted in Figure 4, its behaviour depending on the parameter c. When $0 \leq c < 1$ (case (a)), the BRD always converges towards the equilibrium. When $c = 1$, (Case (b)), then the BRD gets stuck in cycles. The same behaviour is observed when $1 < c \leq 1.5$ (case (c)), except that in this case, all starting points lead to the same cycle. It can moreover be checked that the same behaviour occurs for the synchronous BRD in which $\mathcal{N}_1 = \mathcal{N}_2 = \{1, 2, 3, \ldots\}$, and for the asynchronous BRD.

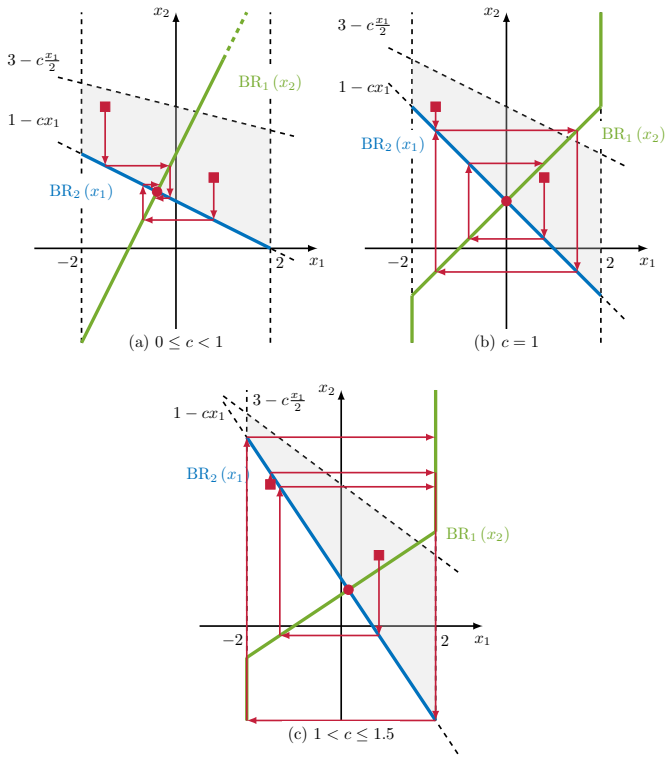


Fig. 4. Illustration of the GNEP of Example 2, for three different parameters c. While the strategy set of the first player is always $[-2; 2]$, the gray area depicts the strategy set of the second player, depending on x_1. The green and blue solid lines correspond respectively to the BR of the first and second player, and their intersection is therefore an equilibrium of the game. For this example, such an equilibrium is always unique, whatever $0 \leq c \leq 1.5$. The sequential BRD is displayed with red arrows, from two different starting points.

Now that the convergence has been assessed visually, conditions provided by Theorem 1 can be investigated. The GNEP has polyhedral strategy sets with variable RHSs, and it fulfils Assumptions 1 to 4. For the objective interaction part, computing the second order derivatives of the objective

© 2024 IEEE. Personal use is permitted, but republication/redistribution requires IEEE permission. See https://www.ieee.org/publications/rights/index.html for more information.

This article has been accepted for publication in IEEE Internet of Things Journal. This is the author's version which has not been fully edited and content may change prior to final publication. Citation information: DOI 10.1109/JIOT.2024.3364756

functions, the convergence matrix reads as

$$\mathbf{\Gamma}^{\text{obj}} = \begin{bmatrix} 0 & c \\ c & 0 \end{bmatrix}.$$

To analyse the constraint set interaction, the player-dependent active constraints sets are computed as $\mathfrak{I}_{12}^{\dagger} = \emptyset$, $\mathfrak{I}_{21}^{\dagger} = \{\{1\},\{2\}\}$. *This gives* $\mathbf{E}_{2,\{1\}} = -1$, $\mathbf{F}_{2,\{1\}} = \mathbf{0}_{0\times 1}$, $\mathbf{G}_{21,\{1\}}(x_1) = c$, *and* $\mathbf{E}_{2,\{2\}} = 1$, $\mathbf{F}_{2,\{2\}} = \mathbf{0}_{0\times 1}$, $\mathbf{G}_{21,\{2\}}(x_1) = \frac{-c}{2}$, *leading to,*

$$\mathbf{\Gamma}_{cons} = \begin{bmatrix} 0 & 0 \\ c & 0 \end{bmatrix}.$$

Finally, one can compute

$$\rho(\mathbf{\Gamma}) = \rho\left(\begin{bmatrix} 0 & c \\ \sqrt{2}c & 0 \end{bmatrix}\right) = \sqrt[4]{2}c,$$

from which one can conclude the asynchronous BRD converges if $c < \frac{1}{\sqrt[4]{2}} \simeq 0.84$. *Comparing this condition with Figure 4, it appears that as expected, the obtained convergence conditions are sufficient but not necessary.*

V. Analysis of the Federated Learning Scenario

In this section, the tools developed in the above section are applied to the FL RA scenario in Section V-A. Then, a numerical analysis validates the obtained theoretical insights in Section V-B.

A. Existence and convergence conditions

To be able to apply the GNEP framework to the FL scenario (6), it must first be checked it belongs to the considered GNEP class. To stick with the generic GNEP notations (7), the objective functions are identified as $u_q(\mathbf{x}_q, \mathbf{x}_{-q}) = \left\|\mathbf{x}_q - \mathbf{x}_q^{(u)}\right\|_2^2$. The inequality constraints of the player-dependent sets $\mathcal{X}_q(\mathbf{x}_q)$ are written in the form of (8), with $\mathcal{I}_q = \{1,\dots,A_q+2\}$,

$$\mathbf{p}_{q,i} = \begin{cases} -\mathbf{e}_i & \forall i = 1,\dots,A_q+1, \\ -\mathbf{w}_q & i = A_q+2, \end{cases}$$

$$\gamma_{q,i}(\mathbf{x}_{-q}) = \begin{cases} x_q^{\max} - 1 & i = 1, \\ 0 & \forall i = 2,\dots,A_q+1, \\ -\frac{R_{\text{up},q}}{\prod_{r\neq q} 1-\mathbb{P}_r+\mathbb{P}_r x_{r,0}} & i = A_q+2, \end{cases}$$

where $\mathbf{e}_i$ is the zero vector with a 1 at the ith index, and $\mathbf{w}_q^{\top} = \left[0, R_{q,1}\mathbb{P}_{\text{cov},1,q}, \dots, R_{q,A_q}\mathbb{P}_{\text{cov},A_q,q}\right]$. The equality constraint leads to $\mathcal{J}_q = \{1\}$, $\tilde{\mathbf{p}}_{q,1} = \mathbf{1}_{A_q+1}$, and $\tilde{\gamma}_{q,1}(\mathbf{x}_{-q}) = 1$. The set of constraints depending on the other players are furthermore defined as $\mathcal{I}_{qr}^{\circ} = \{A_q+2\}$, $\mathcal{J}_{qr}^{\circ} = \emptyset$. Finally, the fixed strategy space $\overline{\mathcal{X}}_q$, always encompassing $\mathcal{X}_q(\mathbf{x}_q)$, is introduced as

$$\overline{\mathcal{X}}_q \triangleq \left\{ \mathbf{x}_q \in \mathbb{R}^{A_q+1} \;\middle|\; \begin{array}{l} x_{q,0} \geq 1 - x_q^{\max}, \\ x_{q,a_q} \geq 0, \quad \forall a_q = 1,\dots,A_q, \\ \sum_{a_q=0}^{A_q} x_{q,a_q} = 1. \end{array} \right\}.$$

Without loss of generality, it is assumed the activity levels are sorted so that the elements of $\mathbf{w}_q$ are increasing. To ensure that Assumptions 1 to 4 hold, and especially to ensure non-emptiness and the Slater constraint qualification, it is sufficient to show that it exists $\nu > 0$ such that the strategy profile $\left[1 - x_q^{\max} + \nu, \nu, \dots, \nu, x_q^{\max} - A_q\nu\right]$ fulfils the minimum rate constraint with a strict inequality, whatever the strategies of the other players. Considering the worst case scenario at which all other players have $x_{r,0} = 1 - x_r^{\max}$, this translates into

$$w_{q,A_q} x_q^{\max} - \nu \sum_{a_q=1}^{A_q} \left(w_{q,A_q} - w_{q,a_q}\right) > \frac{R_{\text{up},q}}{\prod_{r\neq q}(1 - \mathbb{P}_r x_r^{\max})}.$$

A positive ν satisfying the above thus exists for all players if

$$\max_{q=1,\dots,Q} \left\{ \frac{R_{\text{up},q}}{x_q^{\max} R_{q,A_q}\mathbb{P}_{\text{cov},A_q,q}} \frac{1}{\prod_{r\neq q}(1 - \mathbb{P}_r x_r^{\max})} \right\} < 1. \tag{19}$$

The LHS of the above, denoted ρ_{exist}, is named the existence number since as noted above, Assumptions 1 to 3 ensure an equilibrium exists. In the expression of the existence number, $x_q^{\max} R_{q,A_q}\mathbb{P}_{\text{cov},A_q,q}$ is the maximum achievable average rate when no collision occurs, and thus $R_{\text{up},q}/x_q^{\max} R_{q,A_q}\mathbb{P}_{\text{cov},A_q,q}$ depicts the exigence of the FL communication demand compared to the devices' capability. The simplicity of the considered RA scheme comes with an additional $1/\prod_{r\neq q}(1-\mathbb{P}_r x_r^{\max})$ factor, translating the rate loss due to the collisions. Thus, the existence analysis enables to identify a first lever the FL server has to control the interactions.

Lever 1 (Maximum effective rate)**.** *To support an FL scheme targeting a global accuracy* ϵ_g *within a duration* T_g*, the devices must have access to a maximum effective rate* $x_q^{max} R_{q,A_q}\mathbb{P}_{cov,A_q,q}$ *significantly higher than the minimum rate requirement* $R_{up,q}(\epsilon_g, T_g)$.

Now that the existence of an equilibrium is guaranteed, the convergence of the BRD towards this equilibrium must thus be assessed through Theorem 1. As shown in Appendix B, the spectral radius of the convergence matrix is equal to

$$\rho(\mathbf{\Gamma}) = \frac{\sqrt{2}}{\prod_{q=1}^{Q}\left(1 - \mathbb{P}_q x_q^{\max}\right)} \rho(\mathbf{\Theta}),$$

with

$$[\mathbf{\Theta}]_{qr} \triangleq \begin{cases} \frac{\mathbb{P}_q R_{\text{up},q}}{\min\limits_{i=0,\dots,A_q-1} |R_{q,i}\mathbb{P}_{\text{cov},i,q} - R_{q,i+1}\mathbb{P}_{\text{cov},i+1,q}|} & \text{if } r \neq q, \\ 0 & \text{otherwise,} \end{cases}$$

and it can be bounded as [55, Fact 4.10.16]

$$\rho(\mathbf{\Gamma}) \leq \frac{\sqrt{2}}{\prod_{q=1}^{Q}\left(1 - \mathbb{P}_q x_q^{\max}\right)} \max_{\substack{q=1,\dots,Q \\ i=0,\dots,A_q-1}} \left\{ \frac{(Q-1)\,\mathbb{P}_q R_{\text{up},q}}{|R_{q,i}\mathbb{P}_{\text{cov},i,q} - R_{q,i+1}\mathbb{P}_{\text{cov},i+1,q}|} \right\}.$$

Similarly to the existence number, the convergence number is defined as $\rho_{\text{conv}} \triangleq \rho(\mathbf{\Gamma})$. Since Theorem 1 requires the above to be strictly smaller than 1, the following levers are identified.

Lever 2 (Maximum active probability)**.** *The convergence guarantees of the BRD improve when the maximum active probabilities of the devices decrease.*

Lever 3 (Neighbouring activity levels)**.** *The convergence guarantees of the BRD improve when the smallest rate difference between consecutive activity levels* $R_{q,a_q}\mathbb{P}_{cov,a_q,q} -$

© 2024 IEEE. Personal use is permitted, but republication/redistribution requires IEEE permission. See https://www.ieee.org/publications/rights/index.html for more information.

This article has been accepted for publication in IEEE Internet of Things Journal. This is the author's version which has not been fully edited and content may change prior to final publication. Citation information: DOI 10.1109/JIOT.2024.3364756

$R_{q,a_q+1}\mathbb{P}_{cov,a_q+1,q}$, across all devices and activity levels, increases.

As in classical random RA schemes, Lever 2 states that devices should not occupy to many slots, to avoid channel congestion. Lever 3 avoids situations in which a very slight change of probability of the other devices would push the qth worker to switch from the a_qth activity level to the neighbouring one. Doing so, it could impact another device which would do similarly, and the BRD could not converge to an equilibrium. The above levers enable the server to act on the RA parameters (i.e., the maximum active probabilities and the rates of the activity levels) in order to guarantee existence and convergence. In this line of thought, it is interesting to determine how such parameters should scale with the number of players Q, in order to preserve the guarantees, or in other words to keep the existence and convergence numbers unchanged. The below lever identify thus how such scalability should be performed.

Lever 4 (Scalability w.r.t. the number of devices Q)**.** *In order to guarantee the convergence to an equilibrium, the devices' rates should grow in $\mathcal{O}(Q)$, while the maximum active probability should scale as $\mathcal{O}\left(\frac{1}{Q}\right)$.*

As for any multiple access scheme, the above translates the fact that when the number of devices increases, the total communication load also increases. Thus, to keep the communication time constant, the devices should occupy the channel less frequently, but with a higher rate. To support this, the access point should provision a bandwidth proportional to the device number, or loosen the latency constraint T_g.

B. Numerical analysis

To complement and validate the above theoretical analysis, a numerical evaluation is performed in this section. Based on [7], the simulation parameters are selected as follows, except otherwise stated. A model of size $10\,\mathrm{Mb}$ is trained across $Q = 50$ workers, all being selected at each communication round, i.e. $\mathbb{P}_q = 1$ whatever q. The learning process must be finished within $T_g = 10\,\mathrm{min}$, with the centralised step duration $T_0 = 0.33\,\mathrm{s}$ and the duration of one iteration of a local model update $T_{\mathrm{comp},q} = 3.3\,\mathrm{ms}$ whatever q. The local and global accuracies are set to $\epsilon_l = 0.1$, $\epsilon_g = 10^{-2}$, making the number of local iterations and communication rounds equal to $\tau_q = 230$ and $K = 102$, with the model of Figure 2. As discussed above in Lever 4, the bandwidth provisioned by the access point is given by $B = QB_{\mathrm{unit}}$, with $B_{\mathrm{unit}} = 20\,\mathrm{MHz}$. The devices are uniformly located inside a circle of radius $R = 100\,\mathrm{m}$, their distance with respect to the BS being denoted d_q. Their power gain is given by $|h_q|^2 \triangleq \beta d_q^{-\alpha}\zeta_q$, with the path loss intercept $\beta = 34\mathrm{dB}$, the path loss exponent $\alpha = 4$ and the unit-mean fading coefficient ζ_q. Since Rayleigh fading is considered, ζ_q follows an exponential distribution. The noise power spectral density is $\gamma_n = 10^{-15}\mathrm{W/Hz}$. All devices have access to 3 activity levels, with the same power profile $P_{q,a_q} = \gamma_{q,a_q}B$, and $\left[\gamma_{q,a_q}\right]_{a_q=0}^{2} = \left[0, 10^{-10}, \times 10^{-9}\right]$ W/Hz. To achieve a coverage probability of 0.9 for all devices and activity levels, the rates, different across the players, are defined as $R_{q,a_q} = B\log_2\left(1 + \frac{P_{q,a_q}\beta d_q^{-\alpha}}{\gamma_n B\Gamma}\right)$, with $\Gamma = 9.77\,\mathrm{dB}$. The maximum active probability is set to $x_q^{\max} = 1/Q$ for all players. To conclude the devices' description, it remains to specify their interest, modelled by their utopia profile. Considering low-power devices, their objective is to minimise the consumed power, here dependent on the average communication power $\overline{P}_q(\mathbf{x}_q) \triangleq \sum_{a_q=0}^{A_q} x_{q,a_q}P_{q,a_q}$. The utopia profile is then defined as $\mathbf{x}_q^{(u)} = \frac{1}{\epsilon}\left[-P_{q,a_q}\right]_{a_q=0}^{A_q}$ with $\epsilon = 10^{-6}$, as it enables to minimise this average power:

$$\left\|\mathbf{x}_q - \mathbf{x}_q^{(u)}\right\|_2^2 = \left\|\mathbf{x}_q\right\|_2^2 + \left\|\mathbf{x}_q^{(u)}\right\|_2^2 + \frac{2}{\epsilon}\sum_{a_q=0}^{A_q} x_{q,a_q}P_{\mathrm{cons},q,a_q}.$$

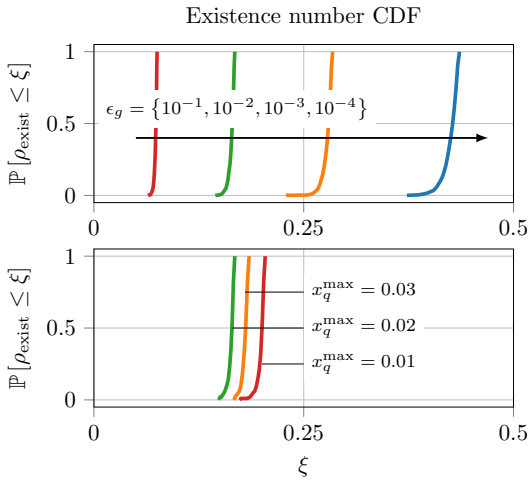


Fig. 5. CDF of the existence number, for different global accuracy requirements and maximum active probability. Existence numbers above 1 would lack existence guarantees, but this does not happen for the considered parameters.

1) Theoretical sufficient conditions: Within this setting, the theoretical conditions guaranteeing the existence of the equilibrium, and the convergence of the BRD towards it, can be assessed across the different worker locations. To that aim, the Cumulative Distribution Function (CDF) of the existence number ρ_{exist} (19), and the one of the convergence number ρ_{conv} are analysed respectively in Figure 5 and Figure 6. The analysis is carried out for different global accuracy losses and maximum active probabilities. As predicted by Levers 1 to 3, the impact of the parameters is as follows. As the accuracy losses decrease (i.e., for more accurate trained models), both the existence and convergence conditions are harder to fulfil. Considering the effect of the maximum active probability on the existence conditions, it appears that both too low and too high probabilities should be avoided. In the first case (low $x_q^{\max}$), the workers might not have the possibility to occupy enough communication slots to be able to transmit the whole model. In the second case (high $x_q^{\max}$), the problem comes from the fact that the other workers might occupy the channel very frequently, resulting in a lot of collisions. This leads to a number of successful communications too low to support the FL task, jeopardising the equilibrium existence. When all devices share the same maximum active probability, from

© 2024 IEEE. Personal use is permitted, but republication/redistribution requires IEEE permission. See https://www.ieee.org/publications/rights/index.html for more information.

This article has been accepted for publication in IEEE Internet of Things Journal. This is the author's version which has not been fully edited and content may change prior to final publication. Citation information: DOI 10.1109/JIOT.2024.3364756

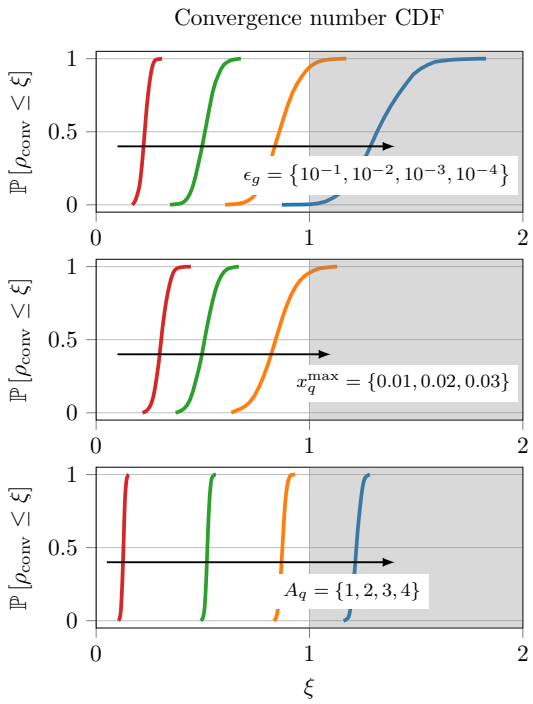


Fig. 6. CDF of the convergence number, for different global accuracy requirements, maximum active probability, and number of activity levels. Convergence numbers greater than 1 do not ensure convergence, as depicted by the gray area.

(19), the optimum value for the existence conditions is at $x_q^{\max} = 1/Q$, which is precisely the default value for this parameter. This is different for the convergence conditions, as increasing the active probability always makes them worse. Finally, the number of activity levels has also been varied, the four following power vectors being considered: $[0, 1]$, $[0, 0.5, 1]$, $[0, 0.33, 0.67, 1]$ and $[0, 0.25, 0.5, 0.75, 1]$ W. As the maximum power is constant, the existence number stays identical for these four profiles, and thus it is not represented. However, as expected and observed in Figure 6, increasing A_q reduces the probability of satisfied convergence conditions.

The above shows that it is critical for the server to tweak the communication levers so as to ensure existence and convergence. Instead of blindly selecting $x_q^{\max} = 1/Q$, the server can among others design the maximum active probability based on the accuracy demand, number of players and available activity levels. For instance, $x_q^{\max}$ can be selected so as to guarantee the two below conditions, with θ and θ' the desired existence and convergence probabilities,

$$\mathbb{P}[\rho_{\text{exist}} < 1] \geq \theta, \qquad \mathbb{P}[\rho_{\text{conv}} < 1] \geq \theta'.$$

As discussed above, this translates in lower and upper bounds on $x_q^{\max}$ for the existence condition, and a lower bound only for the convergence. Any value can then be selected in this range. Figure 7 shows, for different accuracy requirements and number of players, the middle point of this range. This emphasises the link between the FL parameters, and the levers the network designer has in order to make the player interactions converge. As it can be observed in the figure, the selected maximum active probability decreases with the number of players, and with the accuracy requirement. It can also be noticed that when the FL application is too demanding, then no maximum active probability can guarantee at the same time existence and convergence with the desired probabilities.

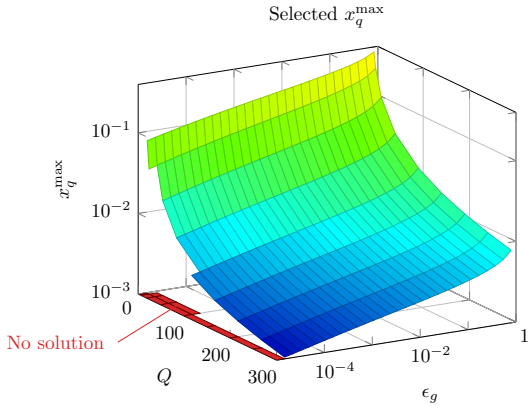


Fig. 7. Selected maximum active probability as a function of the number of players, and accuracy requirement. The selected probability ensures the existence and convergence conditions are satisfied at least with probability $\theta = \theta' = 0.9$. The red area represents the parameters for which there is no maximum active probability satisfying both the existence and convergence conditions.

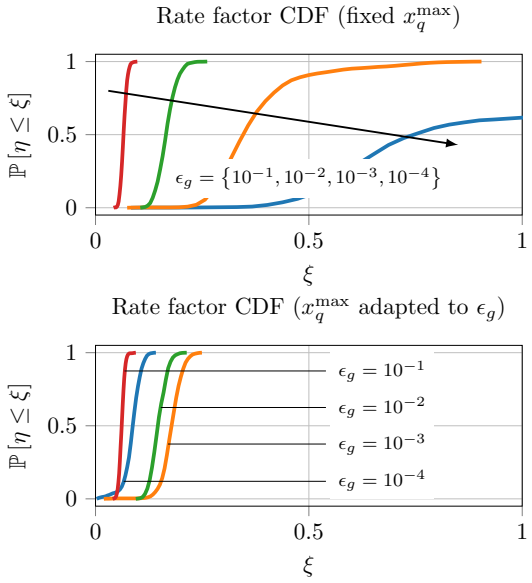


Fig. 8. CDF of the rate factor η, for different global accuracy requirements. On the upper graph, the maximum active probability is set to 0.07, while the bottom graph has this probability adapted to the accuracy loss and power levels.

2) Actual convergence behaviour: Now that the theoretical conditions have been assessed, the impact of the parameters on the actual convergence of the BRD can be investigated. The BRD considered in the FL scheme, described in Algorithm 1, is synchronous when $\mathbb{P}_q = 1$, as it is the case in the numerical simulations. Based on Theorem 1, the convergence rate can then be measured through the rate factor $\eta \triangleq \left\|\mathbf{x}^{(n+1)} - \mathbf{x}^E\right\|_2 / \left\|\mathbf{x}^{(n)} - \mathbf{x}^E\right\|_2$. For the theoretical analysis to be validated, the impact of the parameters on η should mirror their impact on the convergence number ρ_{conv}. Figure 8 and Figure 9

© 2024 IEEE. Personal use is permitted, but republication/redistribution requires IEEE permission. See https://www.ieee.org/publications/rights/index.html for more information.

This article has been accepted for publication in IEEE Internet of Things Journal. This is the author's version which has not been fully edited and content may change prior to final publication. Citation information: DOI 10.1109/JIOT.2024.3364756

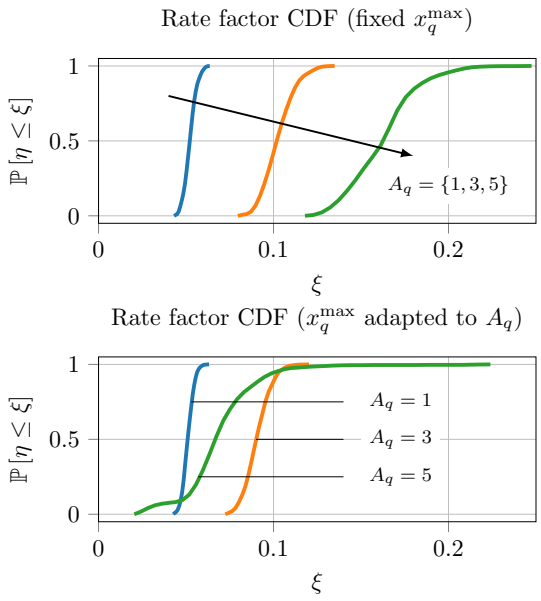


Fig. 9. CDF of the rate factor η, for different number of activity levels, with $\epsilon_g = 2 \cdot 10^{-3}$. On the upper graph, the maximum active probability is set to 0.07, while the bottom graph has this probability adapted to the accuracy loss and power levels.

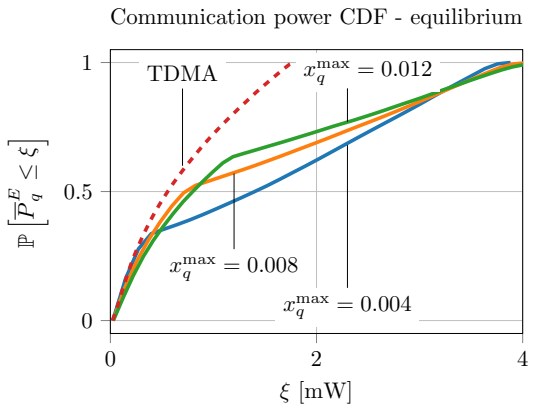


Fig. 10. CDF of the consumed communication power at the equilibrium, for various $x_q^{\max}$, with $\epsilon_g = 10^{-4}$. The value $x_q^{\max} = 0.008$ is the one obtained with Figure 7. The average powers are respectively 1.56 mW, 1.39 mW and 1.32 mW for $x_q^{\max} = 0.004$, 0.008 and 0.012. In the TDMA case, the average power is 0.7 mW.

depict the CDF of η for different accuracy requirements and number of activity levels. As it can be observed in the upper panels, when $x_q^{\max}$ is kept fixed, the CDF of the rate factor shows the same dependency with respect to the parameters as the convergence number, validating the convergence conditions. This dependency is however undesirable, as the goal is to quickly reach a situation at which the rate constraints of all players are satisfied, whatever the FL parameters. In the bottom graphs, $x_q^{\max}$ is thus adapted to ϵ_g and A_q to ensure existence and convergence with high probability. For Figure 8, this is achieved through the relationship depicted in Figure 7, linking the accuracy and player number to the maximum active probability, while a similar relationship has been obtained for A_q, although not represented in the paper. Thus, the bottom panels show that by selecting the maximum active probability through the theoretical conditions, the convergence behaviour becomes almost constant, and consequently holds for a large range of FL parameters.

To conclude this discussion, it should be noted that the above is a proof of concept demonstrating the identified levers enable a control of the interactions. As it is unlikely for the server to have access to a relationship similar to the one of Figure 7, future works should focus on the design of practical algorithms able to select the RA parameters adapted to the FL parameters, based on the above identified levers.

3) Performance at the equilibrium: Now that the theoretical conditions, and the actual BRD convergence, have been numerically assessed, the performance of the FL scheme can be evaluated. From the theoretical guarantees, the rate constraints are known to be fulfilled once the scheme has converged to the equilibrium. It remains to evaluate the objective functions of the workers, their power consumption in this case. To that aim, Figure 10 depicts the CDF of the communication power of the workers, for several maximum active probabilities and with $\epsilon_g = 10^{-4}$. As it can be observed, higher maximum probabilities enable to decrease the power consumption. Indeed, when the maximum active probability is low, the devices have few communication slots to communicate the model and they thus more likely use their maximum power. However, communicating more frequently at a smaller rate is more energy efficient than using few communication slots at a high rate. Therefore, for the same throughput constraint, having higher maximum active probabilities enables to favour more energy efficient solutions.

Figure 10 also depicts the consumed power when the workers communicate in a TDMA manner. In this setting, the workers have access to the channel a fraction $\frac{1}{Q}$ of the time, and must select the power P_{q,a_q} enabling to transmit the whole model within the available time resources. As expected, the power consumed by the active communications is smaller in the TDMA cases, especially in the high power regime. Nevertheless, the advantage in terms of consumed power should be put in balance with the higher complexity of TDMA protocols over RA schemes. For instance, TDMA mechanisms require to perform an allocation of the time resources. This allocation must be communicated to the workers, while it may change at each round if different subsets of workers are selected. To conclude this discussion, it should be noted that the framework developed in this paper precisely enables to reveal such advantages and disadvantages, and to identify levers able to control them. In this case, the carried out analysis shows that the value of $x_q^{\max}$ is such a lever.

4) Comparison with a centralised optimisation: To conclude the analysis, the equilibrium point provided by the BRD can be compared to the global optimum of a centralised optimisation problem. This centralised problem is the minimisation of $\sum_{q=1}^{Q} \left\| \mathbf{x}_q - \mathbf{x}_q^{(u)} \right\|_2^2$ with $\mathbf{x}_q \in \mathcal{X}_q(\mathbf{x}_{-q})$ whatever $q \in \Omega$. Such problem is a convex problem, which must be solved with cone-programming solvers, such as MOSEK, due to the coupled non-linear rate constraints [56]. The global solution $\mathbf{x}^{\text{cent}}$ of this problem can then be compared

© 2024 IEEE. Personal use is permitted, but republication/redistribution requires IEEE permission. See https://www.ieee.org/publications/rights/index.html for more information.

This article has been accepted for publication in IEEE Internet of Things Journal. This is the author's version which has not been fully edited and content may change prior to final publication. Citation information: DOI 10.1109/JIOT.2024.3364756

to the equilibrium point $\mathbf{x}^{\mathrm{E}}$. By jointly considering all devices, the centralised solution is able to control the collision probability, and therefore to favour high activity probability profiles if they enable to reduce the collision probability. In that way, the devices communicate less frequently with a higher power, but the reduce of the collision probability makes this strategy eventually less power hungry. Figure 11 depicts the CDF of the distance between $\mathbf{x}^{\mathrm{E}}$ and $\mathbf{x}^{\mathrm{cent}}$, denoted $\Delta_{\mathbf{x}} \triangleq \frac{1}{Q}\left\|\mathbf{x}^{E}-\mathbf{x}^{\mathrm{cent}}\right\|_2^2$, and the CDF of the relative power consumption excess $P_{\mathrm{rel,exc}} \triangleq \frac{1}{Q}\sum_q \frac{\overline{P}_q^E - \overline{P}_q^{\mathrm{cent}}}{\overline{P}_q^{\mathrm{cent}}}$, for various maximum active probabilities, with $\epsilon_g = 10^{-4}$. As it can be observed, the equilibrium and the centralised solution remain very close to each other, both in terms of distance between the strategies, and of total power consumption. To illustrate this, it is noticed that when using the value given by Figure 7, i.e., $x_q^{\max} = 0.008$, the relative power excess remains below 1% more than 99% of the time. As expected, for greater maximum active probabilities, the power consumption excess increases, even if it remains limited for the considered parameters.

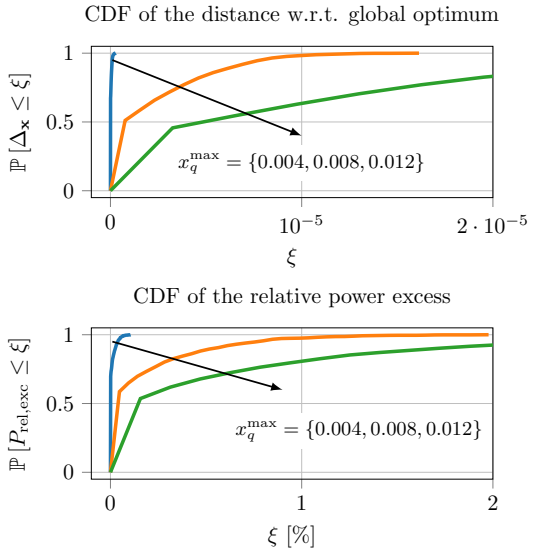


Fig. 11. (Upper panel) Distance CDF between centralised optimum and equilibrium, and (Bottom panel) CDF of the relative power difference. In this figure, $x_q^{\max} = 0.008$ is obtained through Figure 7.

VI. Conclusion

In this work, an FL scenario has been studied, with a focus on the uplink communication step. A slotted multi-activity RA scheme has been designed, in which each node autonomously selects its probability profile. This selected profile is the one closest to a utopia profile, under a minimum rate constraint. This constraint depending on the other workers' choices, the optimisation problems are coupled together, and the resulting interactions have been formulated as an instance of the BRD of a GNEP.

By studying the convergence conditions of the BRD, levers have been identified, guaranteeing that the node interactions converge to an equilibrium. A numerical analysis has been performed, illustrating the identified levers. By studying the performance at the equilibrium, a negligible loss has been observed with respect to the solution of a centralised optimisation.

On the mathematical level, a class of GNEPs has been identified, for which convergence conditions can be obtained for the totally asynchronous BRD. This class is defined by i) the fact that the strategy sets must be polyhedral, with variable right-hand sides, and ii) standard differentiability and convexity assumptions. The sufficient convergence conditions depend on the spectral radius of a convergence matrix, this latter being built in a systematic way from the objective and constraint functions.

Future works include the study of other wireless scenarios calling for a GNEP analysis, which would thus benefit from the developed theoretical framework.

Appendix A
Proof of Theorem 1

The proof of Theorem 1 consists in four steps. First, it is shown in Lemma 1 that the convergence can be linked to the spectral radius of a matrix whose off-diagonal elements are the Lipschitz constants of the BR mappings of the players. Then, Lemma 2 proves that under the considered assumptions, a finite Lipschitz constant exists for each pair of player. Next, Lemma 3 links the Lipschitz constant value to the norm of the gradient of the BR mapping. Finally, Lemma 6 provides an upper-bound on the gradient which only depends on the objective and constraint functions. Throughout the below proof, the lemmas are illustrated on Example 2.

A. Convergence matrix construction

Given the BR mapping of the q-th player $\mathbf{BR}_q(\mathbf{x}_{-q})$ and considering another player r, let L_{qr} be the Lipschitz constant associated with $\mathbf{BR}_q(\mathbf{x}_{-q})$, considering it as a function of the r-th player strategy only. That is, $\forall \left(\mathbf{x}_r, \mathbf{x}_{-(q,r)}\right), \left(\mathbf{y}_r, \mathbf{x}_{-(q,r)}\right) \in \overline{\mathcal{X}}_{-q}$,

$$\left\|\mathbf{BR}_q\left(\mathbf{x}_r, \mathbf{x}_{-(q,r)}\right) - \mathbf{BR}_q\left(\mathbf{y}_r, \mathbf{x}_{-(q,r)}\right)\right\|_2 \leq L_{qr}\left\|\mathbf{x}_r - \mathbf{y}_r\right\|_2,$$

where $\mathbf{x}_{-(q,r)}$ denotes the vector $\overline{\mathbf{x}}$ without the variables of the qth and rth player. Grouping all the constants into the matrix $\mathbf{\Delta} \in \mathbb{R}^{Q\times Q}$, defined as

$$[\mathbf{\Delta}]_{qr} \triangleq \begin{cases} L_{qr} & \text{if } r \neq q, \\ 0 & \text{otherwise,} \end{cases}$$

the following lemma gives a sufficient condition for the BR mapping to be a contraction.

Lemma 1. *The BR mapping* $\mathbf{BR}\colon \overline{\mathcal{X}} \to \overline{\mathcal{X}}$ *satisfies*

$$\left\|\mathbf{BR}(\overline{\mathbf{x}}) - \mathbf{BR}(\overline{\mathbf{y}})\right\|_{\mathbf{\Delta}} \leq \rho(\mathbf{\Delta})\left\|\overline{\mathbf{x}} - \overline{\mathbf{y}}\right\|_{\mathbf{\Delta}}, \quad \forall \overline{\mathbf{x}}, \overline{\mathbf{y}} \in \overline{\mathcal{X}}$$

with $\|\cdot\|_{\mathbf{\Delta}}$ *a well-chosen block-maximum norm. When* $\rho(\mathbf{\Delta}) < 1$*, the BR mapping is thus a contraction of modulus* $\rho(\mathbf{\Delta})$.

Proof. Considering the BR mapping of the first player, given $\mathbf{x}_{-1}, \mathbf{y}_{-1}$, the vectors $\boldsymbol{\xi}^{(r)}$ are defined as

$$\boldsymbol{\xi}^{(r)} = \begin{cases} \mathbf{x}_{-1} & \text{if } r = 2, \\ [\mathbf{y}_2, \ldots, \mathbf{y}_{r-1}, \mathbf{x}_r, \ldots, \mathbf{x}_Q] & \text{if } 3 \leq r \leq Q, \\ \mathbf{y}_{-1} & \text{if } r = Q+1. \end{cases}$$

© 2024 IEEE. Personal use is permitted, but republication/redistribution requires IEEE permission. See https://www.ieee.org/publications/rights/index.html for more information.

This article has been accepted for publication in IEEE Internet of Things Journal. This is the author's version which has not been fully edited and content may change prior to final publication. Citation information: DOI 10.1109/JIOT.2024.3364756

They enable to bound the BR difference as

$$\begin{aligned}
&\|\mathbf{BR}_1(\mathbf{x}_{-1}) - \mathbf{BR}_1(\mathbf{y}_{-1})\|_2 \\
&\quad = \left\| \sum_{r=2}^{Q} \left(\mathbf{BR}_1\left(\xi^{(r)}\right) - \mathbf{BR}_1\left(\xi^{(r+1)}\right) \right) \right\|_2, \\
&\quad \leq \sum_{r=2}^{Q} \left\| \mathbf{BR}_1\left(\xi^{(r)}\right) - \mathbf{BR}_1\left(\xi^{(r+1)}\right) \right\|_2, \\
&\quad \leq \sum_{r=2}^{Q} L_{qr} \|\mathbf{x}_r - \mathbf{y}_r\|_2,
\end{aligned}$$

from the triangular inequality and the definition of the Lipschitz constant L_{qr}, since $\boldsymbol{\xi}^{(r+1)}$ is equal to $\boldsymbol{\xi}^{(r)}$ with $\mathbf{x}_r$ replaced by $\mathbf{y}_r$. Doing so similarly from the other players, and letting $f_q \triangleq \|\mathbf{BR}_q(\mathbf{x}_{-q}) - \mathbf{BR}_q(\mathbf{y}_{-q})\|_2$, $e_q \triangleq \|\mathbf{x}_q - \mathbf{y}_q\|_2$, the following element-wise inequality is obtained

$$\mathbf{0} \leq \mathbf{f} \leq \boldsymbol{\Delta}\mathbf{e}, \quad \forall \mathbf{x}, \mathbf{y} \in \overline{\mathcal{X}}.$$

As it can be shown by following similar steps than those of [3, Appendix C], the above implies the BR is a contraction with modulus $\rho(\boldsymbol{\Delta})$ when such modulus is strictly smaller than 1, under a weighted block-maximum norm depending on $\boldsymbol{\Delta}$. □

The lemma enables to move the focus from the coupled interactions between the Q players together, to the interaction between each couple of players. It remains thus to i) prove the Lipschitz constants L_{qr} exist, and ii) obtain an expression for these constants. Before jumping to the next part of the proof, the lemma is applied to Example 2.

Proof Example - Part 1. *From the expression of the BRs, the Lipschitz constants can be obtained as $L_{12} = L_{21} = c$, leading to $\rho(\boldsymbol{\Delta}) = c$. The lemma ensures thus BRD convergence when $c < 1$, being in this case both sufficient and necessary.*

B. Lipschitz property of the best response mapping

The goal of the the second part of the proof is to show that for all pairs q,r, the BR mapping of the qth player admits a finite Lipschitz constant L_{qr} w.r.t. the strategy of the rth player. To facilitate the proof notations, the optimisation problems of all pairs of players are abstracted into a generic problem $\mathcal{P}_{\mathbf{v}}(\mathbf{t})$ defined as

$$\begin{aligned}
\mathbf{BR}_{\mathbf{v}}(\mathbf{t}) \triangleq \quad & \underset{\mathbf{x}}{\arg\min} \quad u(\mathbf{x}, \mathbf{t}) - \mathbf{x}^\top \mathbf{v}^{(a)} \\
& \text{s.t.} \qquad \mathbf{x} \in \mathcal{X}_{\mathbf{v}}(\mathbf{t}),
\end{aligned} \tag{20}$$

with

$$\mathcal{X}_{\mathbf{v}}(\mathbf{t}) \triangleq \left\{ \mathbf{x} \in \mathbb{R}^n \;\middle|\; \begin{array}{ll} \mathbf{p}_i^\top \mathbf{x} \leq \gamma_i(\mathbf{t}) + v_i^{(b)} & \forall i \in \mathcal{I} \\ \tilde{\mathbf{p}}_j^\top \mathbf{x} = \tilde{\gamma}_j(\mathbf{t}) + v_j^{(c)} & \forall j \in \mathcal{J} \end{array} \right\}.$$

with $\mathcal{I} \triangleq \{1, \ldots, I\}$ and $\mathcal{J} \triangleq \{1, \ldots, J\}$. In the above, $\mathbf{x} \in \mathcal{X} \subseteq \mathbb{R}^n$ mirrors the strategy of the q-th player, $\mathbf{t} \in \mathcal{T} \subseteq \mathbb{R}^m$ the one of the r-th player and $\mathbf{v}^{(a)} \in \mathbb{R}^n$, $\mathbf{v}^{(b)} \in \mathbb{R}^I$, $\mathbf{v}^{(c)} \in \mathbb{R}^J$ are additional perturbations instrumental to the next steps of the proof. The perturbation size is governed by a parameter ϵ since $\mathbf{v} = \left[\mathbf{v}^{(a)}, \mathbf{v}^{(b)}, \mathbf{v}^{(c)}\right]^\top \in \mathcal{V}^\epsilon$ with

$$\mathcal{V}^\epsilon = \left\{ \mathbf{v} \in \mathbb{R}^{n+I+J} \middle| \|\mathbf{v}\|_2 \leq \epsilon \right\}.$$

The set $\mathcal{Z}^\epsilon$ is defined as $\mathcal{Z}^\epsilon = \{(\mathbf{x}, \mathbf{t}, \mathbf{v}) | \mathbf{x} \in \mathcal{X}_{\mathbf{v}}(\mathbf{t}), \mathbf{t} \in \mathcal{T}, \mathbf{v} \in \mathcal{V}^\epsilon\}$, and the sets $\mathcal{I}^\circ \subseteq \mathcal{I}$ and $\mathcal{J}^\circ \subseteq \mathcal{J}$ are moreover introduced as the constraints depending on $\mathbf{t}$, i.e. those for which the RHS function is not constant. Similarly to the game assumptions, the problem family $\mathcal{P}_{\mathbf{v}}(\mathbf{t})$ is assumed to satisfy the following.

Assumption 6.
- *The set $\mathcal{T}$ is compact, convex and non-empty;*
- *The unperturbed strategy set $\mathcal{X}_{\mathbf{0}}(\mathbf{t})$ is bounded, non-empty and fulfils the Slater constraint qualification, $\forall \mathbf{t} \in \mathcal{T}$;*
- *The family $\{\tilde{\mathbf{p}}_j\}_{j \in \mathcal{J}}$ is linearly independent;*
- *The RHS functions $\{\gamma_i(\mathbf{t})\}_{i \in \mathcal{I}}$ and $\{\tilde{\gamma}_j(\mathbf{t})\}_{j \in \mathcal{J}}$ are $\mathcal{C}^1$ in $\mathbf{t}$, $\forall \mathbf{t} \in \mathcal{T}$;*
- *Whatever $(\mathbf{x}, \mathbf{t}, \mathbf{0}) \in \mathcal{Z}^\epsilon$, the objective function $u(\mathbf{x}, \mathbf{t})$ is strongly convex and $\mathcal{C}^2$ in $\mathbf{x}$, and its gradient with respect to $\mathbf{x}$ is $\mathcal{C}^1$ in $\mathbf{t}$.*

Comparing the above assumptions and generic optimisation problem (20) with Assumption 1, it appears the objective function of the players might not be defined, convex, or differentiable on the perturbed set. Yet, the Whitney extension theorem [57] ensures that the objective function of the qth player can be extended outside $\overline{\mathcal{X}}_q$ while keeping a continuous function with continuous derivatives. Since the strong convexity property can be linked to the second derivative information, such extension is strongly convex for ϵ small enough. Hence, the generic objective function $u(\mathbf{x}, \mathbf{t})$ must be understood as the continuously differentiable extension of the player objective functions.

The below lemma then proves that under Assumption 6, a finite Lipschitz constant M_ϵ exists with respect to both $\mathbf{t}$ and $\mathbf{v}$. As a corollary, it proves that for $\mathbf{v} = \mathbf{0}$, a Lipschitz constant L exists with respect to $\mathbf{t}$ only, being the constant needed for the convergence matrix construction. Yet the fact that the BR mapping is Lipschitz also w.r.t $\mathbf{v}$ will be crucial for the next steps of the proof.

Lemma 2. *If Assumption 6 is satisfied, the BR mapping of $\mathcal{P}_{\mathbf{v}}(\mathbf{t})$ admits $M_\epsilon < \infty$ such that $\forall \mathbf{t}, \mathbf{t}' \in \mathcal{T}$, $\forall \mathbf{v}, \mathbf{v}' \in \mathcal{V}^\epsilon$,*

$$\left\| \mathbf{BR}_{\mathbf{v}}(\mathbf{t}) - \mathbf{BR}_{\mathbf{v}'}\left(\mathbf{t}'\right) \right\|_2 \leq M_\epsilon \left\| \begin{array}{c} \mathbf{t} - \mathbf{t}' \\ \mathbf{v} - \mathbf{v}' \end{array} \right\|_2.$$

This implies $\exists L < \infty$ such that $\forall \mathbf{t}, \mathbf{t}' \in \mathcal{T}$,

$$\left\| \mathbf{BR}_{\mathbf{0}}(\mathbf{t}) - \mathbf{BR}_{\mathbf{0}}\left(\mathbf{t}'\right) \right\|_2 \leq L \left\| \mathbf{t} - \mathbf{t}' \right\|_2.$$

Proof. The proof of Lemma 2 consists in two steps. First, it is shown that the boundedness, non-emptiness and constraint qualification assumption of $\mathcal{X}_0(\mathbf{t})$ can be extended to $\mathcal{X}_{\mathbf{v}}(\mathbf{t})$ for small enough perturbations, ensuring the BR mapping is well-defined. Then, the Lipschitz property of the mapping is proved.

For the first part, the boundedness property trivially holds since perturbations are themselves bounded. Then, it is noticed $\mathcal{X}_0(\mathbf{t})$ satisfies the regularity property introduced in [58]. Indeed, the Slater constraint qualification ensures there exists

© 2024 IEEE. Personal use is permitted, but republication/redistribution requires IEEE permission. See https://www.ieee.org/publications/rights/index.html for more information.

This article has been accepted for publication in IEEE Internet of Things Journal. This is the author's version which has not been fully edited and content may change prior to final publication. Citation information: DOI 10.1109/JIOT.2024.3364756

a point $\mathbf{x}$ such that all equality constraints are verified, and all inequality constraints are inactive. Moreover, the equality constraint family $\{\tilde{\mathbf{p}}_j\}_{j\in\mathcal{J}}$ is linearly independent. Then, using successively [58, Corollary 2, Theorem 2], the regularity of $\mathcal{X}_0(\mathbf{t})$ is obtained. From [58, Theorem 1], this implies small enough perturbations leave the system regular, implying in turn the existence of a point leaving the constraints inactive while satisfying the equality constraints. Hence, for ϵ small enough, $\mathcal{X}_{\mathbf{v}}(\mathbf{t})$ is bounded, non-empty and satisfies the Slater constraint qualification.

For the second part, since the optimisation problem $\mathcal{P}_{\mathbf{v}}(\mathbf{t})$ is strongly convex problem and satisfies the Slater constraint qualification, it admits a unique minimiser $\mathbf{BR}_{\mathbf{v}}(\mathbf{t})$ which is also the unique solution of the associated Karush-Kuhn-Tucker (KKT) conditions, for all $(\mathbf{t},\mathbf{v})\in\mathcal{T}\times\mathcal{V}^{\epsilon}$. Moreover, $\mathbf{BR}_{\mathbf{v}}(\mathbf{t})$ satisfies the Mangasarian-Fromovitz constraint qualification since this latter is implied by the Slater constraint qualification and the linear independency of the equality constraints [59], [60]. The constant rank constraint qualification furthermore holds at any point $(\mathbf{x},\mathbf{t},\mathbf{v})\in\mathcal{X}\times\mathcal{T}\times\mathcal{V}^{\epsilon}$ since linear constraints are considered [61]. Therefore, from [62, Theorem 3.6], this implies the BR mapping is Lipschitz continuous w.r.t. $(\mathbf{t},\mathbf{v})$ as the differentiability assumptions of the theorem hold. □

The above lemma ensures that for each pair of player, the constant L_{qr} is finite. The next part of the proof thus focuses on computing this value. Before this, the above lemma is applied to Example 2.

Proof Example - Part 2. *Focusing on the first player, the associated generic optimisation problem is given by*

$$\begin{aligned}\mathrm{BR}_{\mathbf{v}}(t) = \quad & \underset{x}{\arg\min} \quad (x-ct+1)^2 - v_1 x \\ & \text{s.t.} \qquad -2-v_2 \le x \le 2+v_3,\end{aligned}$$

with $t\in\mathcal{T}=[1-2c;3+c]$. To make sure the strategy set remains non-empty, ϵ can for instance be chosen such that $\epsilon\le 0.1$. The associated BR is

$$\mathrm{BR}_{\mathbf{v}}(t)=\min\left\{\max\left\{ct-1+\frac{v_1}{2},-2-v_2\right\},2+v_3\right\}.$$

It can be checked that the above problem satisfies Assumption 6 and that its BR is Lipschitz w.r.t both t and $\mathbf{v}$, as predicted by the lemma.

C. Lipschitz constant as a function of the gradient

Now that a finite Lipschitz constant has been proven to exists, this subsection shows that it can be linked to the gradient of the BR mapping. Hence, the Lipschitz constant, globally measuring how quickly a function varies, is linked to the gradient, locally measuring the rate of change of a function.

To that aim, two sets are introduced, $\operatorname{int}\mathcal{S}$ denoting the interior of the set $\mathcal{S}$. First, $\mathcal{T}_{\mathbf{0}}^{\text{diff}}\triangleq\left\{\bar{\mathbf{t}}\in\operatorname{int}\mathcal{T}\middle|\nabla_{\mathbf{t}}\mathbf{BR}_{\mathbf{0}}(\bar{\mathbf{t}})\text{ exists}\right\}$ is defined as the differentiable points of the unperturbed BR mapping. Then, inspired from [63], the set of well-behaved points is defined as

$$\mathcal{W}^{\epsilon}\triangleq\left\{(\mathbf{t},\mathbf{v})\in\operatorname{int}\mathcal{T}\times\operatorname{int}\mathcal{V}^{\epsilon}\middle|\begin{array}{l}\mathcal{P}_{\mathbf{v}}(\mathbf{t})\text{ has lin. indep. constraints at }\mathbf{BR}_{\mathbf{v}}(\mathbf{t})\\ \text{SCS holds for }\mathcal{P}_{\mathbf{v}}(\mathbf{t})\text{ at }\mathbf{BR}_{\mathbf{v}}(\mathbf{t})\end{array}\right\},$$

with SCS standing for Strict Complementary Slackness. All well-behaved points are such that the BR mapping is differentiable [64], but the converse is not true: $(\mathbf{t},\mathbf{0})\in\mathcal{W}^0 \iff \mathbf{t}\in\mathcal{T}_{\mathbf{0}}^{\text{diff}}$. In the next part, an expression of the gradient will be obtained for the well-behaved point only, this explaining thus why the below lemma considers both $\mathcal{T}_{\mathbf{0}}^{\text{diff}}$ and $\mathcal{W}^{\epsilon}$.

Lemma 3. *The Lipschitz constant L of $\mathbf{BR}_{\mathbf{0}}(\mathbf{t})$ w.r.t $\mathbf{t}$ is given by*

$$\begin{aligned}L=&\sup_{\bar{\mathbf{t}}\in\mathcal{T}_{\mathbf{0}}^{\text{diff}}}\sigma_{\max}\left(\nabla_{\mathbf{t}}\mathbf{BR}_{\mathbf{0}}(\bar{\mathbf{t}})\right)\\ &\le\lim_{\epsilon\to0^+}\sup_{(\bar{\mathbf{t}},\bar{\mathbf{v}})\in\mathcal{W}^{\epsilon}}\sigma_{\max}\left(\nabla_{\mathbf{t}}\mathbf{BR}_{\bar{\mathbf{v}}}(\bar{\mathbf{t}})\right).\end{aligned}$$

Proof. From Lemma 2, the unperturbed BR mapping $\mathbf{BR}_{\mathbf{0}}(\mathbf{t})$ is Lipschitz continuous. Thus, for all $\bar{\mathbf{t}}\in\operatorname{int}\mathcal{T}$, its Clarke generalised gradient is defined as [65], [66]:

$$\begin{aligned}\overline{\nabla}_{\mathbf{t}}\mathbf{BR}_{\mathbf{0}}(\bar{\mathbf{t}})\triangleq\operatorname{con}\big\{&\mathbf{A}\in\mathbb{R}^{n\times m}\big|\\ &\exists\mathbf{t}^{\rho}\to\bar{\mathbf{t}}\text{ with }\mathbf{t}^{\rho}\in\mathcal{T}_{\mathbf{0}}^{\text{diff}},\nabla_{\mathbf{t}}\mathbf{BR}_{\mathbf{0}}(\mathbf{t}^{\rho})\to\mathbf{A}\big\}.\end{aligned}$$

The Lipschitz constant on $\operatorname{int}\mathcal{T}$ is then obtained as

$$L=\sup_{\bar{\mathbf{t}}\in\operatorname{int}\mathcal{T}}\max_{\mathbf{A}\in\overline{\nabla}_{\mathbf{t}}\mathbf{BR}_{\mathbf{0}}(\bar{\mathbf{t}})}\sigma_{\max}(\mathbf{A}),$$

from successively [67, Theorem 9.2, Proposition 9.24, Theorem 9.6.2] and the fact that the matrix norm induced by the vector euclidean norm is the maximum singular value of the matrix. Since [67, Theorem 9.58 and 2.33] shows that points in $\mathcal{T}\setminus\operatorname{int}\mathcal{T}$ do not modify the Lipshitz constant, the above is valid for $\mathcal{T}$, including its boundary. Since the generalised gradient is a limit point of a sequence of gradients at the differentiable points, the equality part of Lemma 3 is obtained.

Considering only well-behaved points in the above Clarke generalised gradient definition does not work. Indeed, the ill-behaved points (those which are not well-behaved) are not negligible in $\operatorname{int}\mathcal{T}$, the negligibility property being defined in [63]. Whatever $\mathbf{t}\in\operatorname{int}\mathcal{T}$, fixed, the set of ill-behaved point is however negligible in $\operatorname{int}\mathcal{V}^{\epsilon}$, since the differentiability assumptions of [63] are satisfied. This in turn implies that the set of ill-behaved points is negligible in $\operatorname{int}\mathcal{T}\times\operatorname{int}\mathcal{V}^{\epsilon}$. The projected generalised gradient of the BR mapping with respect to $\mathbf{t}$ at $(\bar{\mathbf{t}},\mathbf{0})\in\operatorname{int}\mathcal{T}\times\operatorname{int}\mathcal{V}^{\epsilon}$ can then be defined as

$$\begin{aligned}&\boldsymbol{\pi}_{\mathbf{t}}\overline{\nabla}\mathbf{BR}_{\mathbf{0}}(\bar{\mathbf{t}})\\ &\quad\triangleq\operatorname{con}\big\{\mathbf{A}\in\mathbb{R}^{n\times m}\big|\,\exists(\mathbf{t}^{\rho},\mathbf{v}^{\rho})\to(\bar{\mathbf{t}},\mathbf{0})\\ &\qquad\text{with }(\mathbf{t}^{\rho},\mathbf{v}^{\rho})\in\mathcal{W}^{\epsilon},\nabla_{\mathbf{t}}\mathbf{BR}_{\mathbf{v}^{\rho}}(\mathbf{t}^{\rho})\to\mathbf{A}\big\},\end{aligned}$$

where the sequence of converging gradient is allowed to explore the perturbations. The meaning of the $\boldsymbol{\pi}_{\mathbf{t}}\overline{\nabla}\mathbf{BR}_{\mathbf{0}}(\bar{\mathbf{t}})$ notation is that first the generalised gradient with respect to both $\mathbf{t}$ and $\mathbf{v}$ is computed as $\overline{\nabla}\mathbf{BR}_{\mathbf{0}}(\bar{\mathbf{t}})$, and then only the $\mathbf{t}$ part is kept through the $\boldsymbol{\pi}_{\mathbf{t}}$ operator. Such projected gradient satisfies [66, Proposition 2.3.16]

$$\overline{\nabla}_{\mathbf{t}}\mathbf{BR}_{\mathbf{0}}(\bar{\mathbf{t}})\subseteq\boldsymbol{\pi}_{\mathbf{t}}\overline{\nabla}\mathbf{BR}_{\mathbf{0}}(\bar{\mathbf{t}}),$$

and thus the inequality part of the lemma is obtained. □

© 2024 IEEE. Personal use is permitted, but republication/redistribution requires IEEE permission. See https://www.ieee.org/publications/rights/index.html for more information.

This article has been accepted for publication in IEEE Internet of Things Journal. This is the author's version which has not been fully edited and content may change prior to final publication. Citation information: DOI 10.1109/JIOT.2024.3364756

In the next part of the proof, Lemma 4 provides an expression of the BR gradient directly from the objective and constraint functions. Yet, such expression is only valid for the well-behaved points, and not all differentiable points. This explains why $\mathcal{W}^\epsilon$ is introduced, although only providing an upper-bound on the Lipschitz constant. Before moving to the next part of the proof, the above lemma is applied to Example 2.

Proof Example - Part 3. *For the first player, the set of differentiable points is obtained as* $\mathcal{T}_{\mathbf{0}}^{\text{diff}} = \operatorname{int}\mathcal{T} \setminus \left\{\frac{-1}{c}, \frac{3}{c}\right\}$, *and thus*

$$L = \sup_{\bar{t}\in\mathcal{T}_{\mathbf{0}}^{\text{diff}}} \left|\nabla_t \text{BR}_{\mathbf{0}}\left(\bar{t}\right)\right| = \max\left\{0, c, 0\right\} = c.$$

To identify the well-behaved points, the KKT triplet is obtained as

$$\begin{aligned}
&\left(\text{BR}_{\mathbf{v}}\left(t\right), \mu^t_{\mathbf{v},1}, \mu^t_{\mathbf{v},2}\right) \\
&= \begin{cases} (-2-v_2, -2-2ct-v_1-2v_2, 0) \\ \qquad\qquad \textit{if } ct \leq -1-\frac{v_1}{2}-v_2, \\ \left(ct-1+\frac{v_1}{2}, 0, 0\right) \\ \qquad\qquad \textit{otherwise}, \\ (2+v_3, 2ct-6+v_1-2v_3, 0) \\ \qquad\qquad \textit{if } ct \geq 3-\frac{v_1}{2}+v_3, \end{cases}
\end{aligned}$$

with $\mu^t_{\mathbf{v},1}$ *and* $\mu^t_{\mathbf{v},2}$ *the multipliers associated with the first and second constraint. There exists no* $(\mathbf{t}, \mathbf{v})$ *for which the linear independency does not hold, but there exist points at which both the multiplier is zero and the associated constraint is active, i.e. points at which the strict complementary slackness does not hold:*

$$\mathcal{W}^\epsilon = \left\{(t, \mathbf{v}) \in \operatorname{int}\mathcal{T} \times \operatorname{int}\mathcal{V}^\epsilon \,\middle|\, \begin{cases} ct + \frac{v_1}{2} + v_2 & \neq & -1 \\ ct + \frac{v_1}{2} - v_3 & \neq & 3 \end{cases}\right\}.$$

The Lipschitz upper-bound, being exact in this case, is thus obtained as

$$L \leq \lim_{\epsilon\to 0^+} \sup_{(\bar{t},\bar{\mathbf{v}})\in\mathcal{W}^\epsilon} \left|\nabla_t \text{BR}_{\bar{\mathbf{v}}}\left(\bar{t}\right)\right| = \max\left\{0, c, 0\right\} = c.$$

D. Gradient expression from the optimisation problem

This last step of the proof obtains an expression of the gradient from the objective and constraint functions. To that aim, the second-order derivatives of the objective function are introduced as

$$\begin{aligned}
\mathbf{H}\left(\mathbf{x}, \mathbf{t}\right) &= \boldsymbol{\nabla}^2_{\mathbf{xx}} u\left(\mathbf{x}, \mathbf{t}\right) \in \mathbb{R}^{n\times n}, \\
\mathbf{K}\left(\mathbf{x}, \mathbf{t}\right) &= \boldsymbol{\nabla}^2_{\mathbf{xt}} u\left(\mathbf{xt}\right) \in \mathbb{R}^{n\times m}.
\end{aligned}$$

On the constraint side, the set of active inequality constraints at $(\mathbf{x}, \mathbf{t}, \mathbf{v})$ is denoted as $\mathcal{I}^{\mathbf{t}}_{\mathbf{v}}\left(\mathbf{x}\right) \triangleq \left\{i \in \mathcal{I} \middle| \mathbf{p}_i^\top \mathbf{x} = \gamma_i\left(\mathbf{t}\right) + v_i^{(b)}\right\}$ and the total number of active constraints as $r^{\mathbf{t}}_{\mathbf{v}}\left(\mathbf{x}\right) \triangleq \left|\mathcal{I}^{\mathbf{t}}_{\mathbf{v}}\left(\mathbf{x}\right)\right| + J$. Then, the first-order constraint derivatives are grouped into the matrices

$$\begin{aligned}
\mathbf{P}_{\mathcal{I}^{\mathbf{t}}_{\mathbf{v}}(\mathbf{x})} &\triangleq \begin{bmatrix} \left\{\mathbf{p}_i^\top\right\}_{i\in\mathcal{I}^{\mathbf{t}}_{\mathbf{v}}(\mathbf{x})} \\ \left\{\tilde{\mathbf{p}}_j^\top\right\}_{j\in\mathcal{J}} \end{bmatrix} \in \mathbb{R}^{r^{\mathbf{t}}_{\mathbf{v}}(\mathbf{x})\times n}, \\
\mathbf{S}_{\mathcal{I}^{\mathbf{t}}_{\mathbf{v}}(\mathbf{x})}\left(\mathbf{t}\right) &\triangleq \begin{bmatrix} \left\{\boldsymbol{\nabla}_{\mathbf{t}}^\top \gamma_i\left(\mathbf{t}\right)\right\}_{i\in\mathcal{I}^{\mathbf{t}}_{\mathbf{v}}(\mathbf{x})} \\ \left\{\boldsymbol{\nabla}_{\mathbf{t}}^\top \tilde{\gamma}_j\left(\mathbf{t}\right)\right\}_{j\in\mathcal{J}} \end{bmatrix} \in \mathbb{R}^{r^{\mathbf{t}}_{\mathbf{v}}(\mathbf{x})\times m}.
\end{aligned}$$

Merging the objective and constraints part, the following idempotent matrices are defined as

$$\begin{aligned}
&\mathbf{R}\left(\mathbf{x}, \mathbf{t}, \mathbf{v}\right) \\
&\triangleq \begin{cases} \left[\mathbf{I}_n - \mathbf{H}^{-1}\mathbf{P}^\top\left(\mathbf{P}\mathbf{H}^{-1}\mathbf{P}^\top\right)^+\mathbf{P}\right]_{(\mathbf{x},\mathbf{t},\mathbf{v})} & \text{if } r^{\mathbf{t}}_{\mathbf{v}}\left(\mathbf{x}\right) > 0, \\ \mathbf{I}_n & \text{otherwise}, \end{cases} \\
&\mathbf{R}_\perp\left(\mathbf{x}, \mathbf{t}, \mathbf{v}\right) \triangleq \mathbf{I}_n - \mathbf{R}\left(\mathbf{x}, \mathbf{t}, \mathbf{v}\right),
\end{aligned}$$

where $(\cdot)^+$ denotes the generalised inverse operator while $[\cdot]_{\mathbf{z}}$ means that all matrices inside the brackets are evaluated at $\mathbf{z}$. With these definitions, the gradient of the BR mapping is obtained in the following lemma.

Lemma 4. *The gradient of* $\mathbf{BR}_{\mathbf{v}}\left(\mathbf{t}\right)$ *with respect to* $\mathbf{t}$ *at a point* $(\mathbf{t}, \mathbf{v}) \in \mathcal{W}^\epsilon$ *is given by*

$$\boldsymbol{\nabla}_{\mathbf{t}}\mathbf{BR}_{\mathbf{v}}\left(\mathbf{t}\right) = \left[-\mathbf{R}\mathbf{H}^{-1}\mathbf{K} + \mathbf{R}_\perp\mathbf{P}^+\mathbf{S}\right]_{(\mathbf{BR}_{\mathbf{v}}(\mathbf{t}),\mathbf{t},\mathbf{v})}.$$

Proof. The above is a direct consequence of [64, Section 4], showing that for well-behaved points,

$$\begin{aligned}
&\boldsymbol{\nabla}_{\mathbf{t}}\mathbf{BR}_{\mathbf{v}}\left(\mathbf{t}\right) \\
&\quad = \left[-\mathbf{R}\mathbf{H}^{-1}\mathbf{K} + \mathbf{H}^{-1}\mathbf{P}^\top\left(\mathbf{P}\mathbf{H}^{-1}\mathbf{P}^\top\right)^{-1}\mathbf{S}\right]_{(\mathbf{BR}_{\mathbf{v}}(\mathbf{t}),\mathbf{t},\mathbf{v})}.
\end{aligned}$$

When no constraint is active, the second term of the above is $\mathbf{0}$. When at least one is active, since at well-behaved points the linear independence of the constraints holds, $\mathbf{P}$ is full-row rank and thus a factor $\mathbf{P}\mathbf{P}^+ = \mathbf{I}$ can be introduced to make $\mathbf{R}_\perp$ appear. □

Due to the intricate expression of $\mathbf{R}$, computing the maximum singular value of the above over all possible $(\mathbf{t}, \mathbf{v})$ is challenging, although required by Lemma 3. Hence, the below lemma simplifies the expression and discards the dependency on the idempotent matrix $\mathbf{R}^{\mathbf{t}}_{\mathbf{v}}$. It also leverages the fact that for the constraints independent of $\mathbf{t}$, the lines of $\mathbf{S}$ are $\mathbf{0}$. To take into account this fact, the rows of $\mathbf{P}$ and $\mathbf{S}$ are permuted and partitioned as

$$\mathbf{P} = \begin{bmatrix} \mathbf{E} \\ \mathbf{F} \end{bmatrix}, \quad \text{and} \quad \mathbf{S} = \begin{bmatrix} \mathbf{G} \\ \mathbf{0} \end{bmatrix},$$

with $\mathbf{E}$ and $\mathbf{G}$ be the lines of the constraints dependent on $\mathbf{t}$, and $\mathbf{F}$ those of the fixed ones. The projector onto the null space of $\mathbf{F}$ is moreover introduced as $\boldsymbol{\Pi} = \mathbf{I}_n - \mathbf{F}^\top\left(\mathbf{F}\mathbf{F}^\top\right)^{-1}\mathbf{F}$, being well-defined for the well-behaved points.

Lemma 5. *The maximum singular value of the gradient of* $\mathbf{BR}_{\mathbf{v}}\left(\mathbf{t}\right)$ *with respect to* $\mathbf{t}$ *at a point* $(\mathbf{t}, \mathbf{v}) \in \mathcal{W}^\epsilon$ *is bounded by*

$$\begin{aligned}
&\sigma_{\max}\left(\boldsymbol{\nabla}_{\mathbf{t}}\mathbf{BR}_{\mathbf{v}}\left(\mathbf{t}\right)\right) \\
&\quad \leq \left[\sqrt{\frac{\sigma^2_{\max}\left(\mathbf{K}\right)}{\lambda^2_{\min}\left(\mathbf{H}\right)} + \kappa\left(\mathbf{H}\right)\sigma^2_{\max}\left(\left(\mathbf{E}\boldsymbol{\Pi}\right)^+\mathbf{G}\right)}\right]_{(\mathbf{BR}_{\mathbf{v}}(\mathbf{t}),\mathbf{t},\mathbf{v})}.
\end{aligned}$$

Proof. The positive definite matrix $\mathbf{H}$ is factorised as $\mathbf{H}^{-1} = \mathbf{L}\mathbf{L}^\top$. Defining $\tilde{\mathbf{R}} = \mathbf{L}^{-1}\mathbf{R}\mathbf{L}$ and $\tilde{\mathbf{R}}_\perp = \mathbf{I}_n - \tilde{\mathbf{R}}$, these matrices are idempotent and symmetric (i.e., they are projectors). This enables to bound them as $\sigma^2_{\max}\left(\begin{bmatrix}\tilde{\mathbf{R}} & \tilde{\mathbf{R}}_\perp\end{bmatrix}\right) =$

© 2024 IEEE. Personal use is permitted, but republication/redistribution requires IEEE permission. See https://www.ieee.org/publications/rights/index.html for more information.

This article has been accepted for publication in IEEE Internet of Things Journal. This is the author's version which has not been fully edited and content may change prior to final publication. Citation information: DOI 10.1109/JIOT.2024.3364756

$\lambda_{\max}\left(\tilde{\mathbf{R}}\tilde{\mathbf{R}}^\top + \tilde{\mathbf{R}}_\perp\tilde{\mathbf{R}}_\perp^\top\right) = \lambda_{\max}(\mathbf{I}_n) = 1$. Then, from [55, Cor. 9.6.4, Fact 9.14.14]

$$\begin{aligned}
&\sigma_{\max}\left(-\mathbf{R}\mathbf{H}^{-1}\mathbf{K} + \mathbf{R}_\perp\mathbf{P}^+\mathbf{S}\right)\\
&\quad= \sigma_{\max}\left(\mathbf{L}\begin{bmatrix}\tilde{\mathbf{R}} & \tilde{\mathbf{R}}_\perp\end{bmatrix}\begin{bmatrix}-\mathbf{L}^\top\mathbf{K}\\ \mathbf{L}^{-1}\mathbf{P}^+\mathbf{S}\end{bmatrix}\right),\\
&\quad\leq \sigma_{\max}(\mathbf{L})\sqrt{\sigma^2_{\max}(\mathbf{L}^\top\mathbf{K}) + \sigma^2_{\max}(\mathbf{L}^{-1}\mathbf{P}^+\mathbf{S})},\\
&\quad\leq \sigma_{\max}(\mathbf{L})\sqrt{\sigma^2_{\max}(\mathbf{L})\,\sigma^2_{\max}(\mathbf{K}) + \sigma^2_{\max}(\mathbf{L}^{-1})\,\sigma^2_{\max}(\mathbf{P}^+\mathbf{S})},\\
&\quad= \sqrt{\frac{\sigma^2_{\max}(\mathbf{K})}{\lambda^2_{\min}(\mathbf{H})} + \kappa(\mathbf{H})\,\sigma^2_{\max}(\mathbf{P}^+\mathbf{S})}.
\end{aligned}$$

From [55, Fact 6.1.6.xxx], any permutation matrix $\mathbf{\Sigma}$ is such that $\mathbf{P}^+\mathbf{S} = (\mathbf{\Sigma}\mathbf{P})^+\mathbf{\Sigma}\mathbf{S}$, showing that the rows of $\mathbf{P}$ and $\mathbf{S}$ can be permuted with the same performutation. This thus makes the $\mathbf{E}$, $\mathbf{F}$ and $\mathbf{G}$ submatrices appear, leading to, from [55, Fact 6.1.6, 6.5.18, 2.17.3],

$$\begin{aligned}
\mathbf{P}^+\mathbf{S} &= \begin{bmatrix}\mathbf{E}\\ \mathbf{F}\end{bmatrix}^+\begin{bmatrix}\mathbf{G}\\ \mathbf{0}\end{bmatrix}\\
&= \begin{bmatrix}\mathbf{E}^\top\\ \mathbf{F}\top\end{bmatrix}\begin{bmatrix}\mathbf{E}\mathbf{E}^\top & \mathbf{E}\mathbf{F}^\top\\ \mathbf{F}\mathbf{E}^\top & \mathbf{F}\mathbf{F}^\top\end{bmatrix}^{-1}\begin{bmatrix}\mathbf{G}\\ \mathbf{0}\end{bmatrix},\\
&= \left[\mathbf{E}^\top\left(\mathbf{E}\mathbf{\Pi}\mathbf{E}^\top\right)^{-1} - (\mathbf{I}_n - \mathbf{\Pi})\,\mathbf{E}^\top\left(\mathbf{E}\mathbf{\Pi}\mathbf{E}^\top\right)^{-1}\right]\mathbf{G}\\
&= (\mathbf{E}\mathbf{\Pi})^+\mathbf{G},
\end{aligned}$$

concluding the proof. □

The expression provided by Lemma 5 still depends on the optimisation problem solution $\mathbf{BR}_{\mathbf{v}}(\mathbf{t})$ which is in general not known. Moreover, the impact of the vanishingly small perturbations is not clear from the above expression. To circumvent this, the following set is introduced, grouping all possible sets of linearly independent active constraints, with at least one depending on $\mathbf{t}$:

$$\mathfrak{J}^\dagger = \left\{\tilde{\mathcal{I}}\;\middle|\;\begin{array}{l}\forall\epsilon>0, \exists(\mathbf{x},\mathbf{t},\mathbf{v})\in\mathcal{Z}^\epsilon \text{ s.t. } \tilde{\mathcal{I}} = \mathcal{I}^{\mathbf{t}}_{\mathbf{v}}(\mathbf{x})\\ \left\{\{\mathbf{p}_i\}_{i\in\tilde{\mathcal{I}}}, \{\tilde{\mathbf{p}}_j\}_{j\in\mathcal{J}}\right\} \text{ is linearly independent}\\ \tilde{\mathcal{I}}\cap\mathcal{I}^\circ\neq\emptyset \text{ or } \mathcal{J}\cap\mathcal{J}^\circ\neq\emptyset\end{array}\right\}.$$

From the above definition, it can be noticed that for problems for which Assumption 4 holds, the above can be defined with $\mathbf{v} = \mathbf{0}$ without loss of generality.

Lemma 6. *The Lipschitz constant of* $\mathbf{BR_0}(\mathbf{t})$ *w.r.t* $\mathbf{t}$ *is bounded by*

$$\begin{aligned}
L^2 \leq &\max_{\substack{\mathbf{t}\in\mathcal{T}\\ \mathbf{x}\in\mathcal{X_0}(\mathbf{t})}}\left\{\frac{\sigma^2_{\max}(\mathbf{K})}{\lambda^2_{\min}(\mathbf{H})}\right\}\\
&+\max_{\substack{\mathbf{t}\in\mathcal{T}\\ \mathbf{x}\in\mathcal{X_0}(\mathbf{t})}}\{\kappa(\mathbf{H})\}\max_{\substack{\tilde{\mathcal{I}}\in\mathfrak{J}^\dagger\\ \mathbf{t}\in\mathcal{T}}}\left\{\sigma^2_{\max}\left((\mathbf{E}\mathbf{\Pi})^+\mathbf{G}\right)\right\}.
\end{aligned}$$

Proof. Considering the worst case active constraint set instead of the actual one, the Lipschitz constant is upper-bounded as

$$\begin{aligned}
L^2 \leq &\lim_{\epsilon\to0^+}\sup_{\substack{(\mathbf{t},\mathbf{v})\in\mathcal{W}^\epsilon\\ \mathbf{x}=\mathbf{BR_v}(\mathbf{t})}}\frac{\sigma^2_{\max}(\mathbf{K})}{\lambda^2_{\min}(\mathbf{H})}\\
&+\kappa(\mathbf{H})\max_{\tilde{\mathcal{I}}\in\mathfrak{J}^\dagger}\left\{\sigma^2_{\max}\left((\mathbf{E}\mathbf{\Pi})^+\mathbf{G}\right)\right\}.
\end{aligned}$$

From the continuity of the BR mapping, of the derivatives, and of the maximum singular value and minimum eigenvalue operators, the above expression is continuous in both $\mathbf{t}$ and $\mathbf{v}$. Therefore, the vanishingly small perturbations can be discarded, and the whole set $\mathcal{T}$ can be considered. This leads to

$$\begin{aligned}
L^2 \leq &\max_{\substack{\mathbf{t}\in\mathcal{T}\\ \mathbf{x}=\mathbf{BR_0}(\mathbf{t})}}\frac{\sigma^2_{\max}(\mathbf{K})}{\lambda^2_{\min}(\mathbf{H})} + \kappa(\mathbf{H})\max_{\tilde{\mathcal{I}}\in\mathfrak{J}^\dagger}\left\{\sigma^2_{\max}\left((\mathbf{E}\mathbf{\Pi})^+\mathbf{G}\right)\right\}.
\end{aligned}$$

Since $\mathbf{BR_0}(\mathbf{t})$ is yet difficult to obtain in closed form and to maximise upon, the maximum is instead taken over all $\mathbf{x}\in\mathcal{X_0}(\mathbf{t})$, concluding the proof of Lemma 6. □

Proof Example - Part 4. *The first player optimisation problem is such that* $\mathfrak{J}^\dagger = \emptyset$ *since no constraint depends on* $\mathbf{t}$*, and therefore the second term can be ignored. The Lipschitz constant upper-bound is thus given by*

$$L \leq \max_{\substack{t\in[1-2c\,;\,3+c]\\ x\in[-2\,;\,2]}}\left\{\frac{|-2c|}{2}\right\} = c,$$

the bound being in this case exact. For the second player, $\mathfrak{J}^\dagger = \{\{1\},\{2\}\}$*. Therefore,*

$$L \leq \sqrt{\max_{\substack{t\in[-2\,;\,2]\\ x\in\left[1-ct\,;\,3-c\frac{t}{2}\right]}}\left\{\frac{(2c)^2}{2^2}\right\} + \max\left\{\frac{c^2}{4}, c^2\right\}} = \sqrt{2}c.$$

In this case, the upper-bound overestimates the actual Lipschitz constant.

APPENDIX B
CONVERGENCE CONDITIONS FOR THE FEDERATED LEARNING SCENARIO

First, it is noticed that as there is no objective function interactions, $\mathbf{\Gamma}^{\text{obj}} = \mathbf{0}$ and thus one can focus on the constraint part. Moreover, the 2-norm objective leads to $\nabla^2_{\mathbf{x}_q\mathbf{x}_q}u_q(\overline{\mathbf{x}}) = \mathbf{I}$ for all workers, with the associated condition number equal to 1. It remains to look at the linearly independent constraints sets which can be active at the same time, with at least one constraint depending on the other players. Such sets always include the (A_q+2)th constraint since it is the only one depending on the other players. To preserve a linearly independent set, considering an active (A_q+2)th constraint and the active equality constraint, only A_q-1 lower bounds can be active at the same time. Therefore,

$$\mathfrak{J}^\dagger_{qr} = \{\mathcal{S}\subseteq\{1,\dots,A_q+1\}||\mathcal{S}|\leq A_q-1\}\cup\{A_q+2\}.$$

In the above, one could refine the definition of $\mathfrak{J}^\dagger_{qr}$ by studying which lower bound sets could never be jointly active. Yet, this is challenging and such result would typically depend on $\mathbf{x}_q^{(u)}$, and thus this direction is not pursued here. Given $\mathcal{I}\in\mathfrak{J}^\dagger_{qr}$, the indices of the active lower-bounds are defined as $\mathcal{I}^{\text{a}} \triangleq \mathcal{I}\setminus\{A_q+2\}$ and their number is denoted by $N \triangleq |\mathcal{I}|-1$. The variables not constrained by the lower bounds are indexed in $\mathcal{I}^{\text{Na}} = \{1,\dots,A_q+1\}\setminus\mathcal{I}^{\text{a}}$, and their number is defined as $m \triangleq A_q+1-N$. The elements of $\mathbf{w}_q$ related respectively to the variables constrained by the lower bounds, and those for which

© 2024 IEEE. Personal use is permitted, but republication/redistribution requires IEEE permission. See https://www.ieee.org/publications/rights/index.html for more information.

This article has been accepted for publication in IEEE Internet of Things Journal. This is the author's version which has not been fully edited and content may change prior to final publication. Citation information: DOI 10.1109/JIOT.2024.3364756

it is not the case, are grouped into $\mathbf{w}_{q,\mathcal{I}^{\mathrm{a}}}$ and $\mathbf{w}_{q,\mathcal{I}^{\mathrm{Na}}}$. With these definitions, the matrices instrumental to the definition of the convergence matrix are obtained as

$$\mathbf{E}_{qr,\mathcal{I}} = \begin{bmatrix} -\mathbf{w}_{q,\mathcal{I}^{\mathrm{a}}} & -\mathbf{w}_{q,\mathcal{I}^{\mathrm{Na}}} \end{bmatrix}, \quad \mathbf{F}_{qr,\mathcal{I}} = \begin{bmatrix} -\mathbf{I}_N & \mathbf{0}_{N\times m} \\ \mathbf{1}_N^\top & \mathbf{1}_m^\top \end{bmatrix},$$
$$\mathbf{G}_{qr,\mathcal{I}}\left(\mathbf{x}_{-q}\right) = \left[\frac{R_{\mathrm{up},q}}{\prod_{p\neq q}(1-\mathbb{P}_p+\mathbb{P}_p x_{p,0})} \frac{\mathbb{P}_r}{(1-\mathbb{P}_r+\mathbb{P}_r x_{r,0})}, 0, \ldots, 0 \right].$$

With respect to the definition provided in Theorem 1, one can notice that the columns of $\mathbf{E}_{qr,\mathcal{I}}$ and $\mathbf{F}_{qr,\mathcal{I}}$ have been permuted for the sake of simplicity, since permutation matrices can be introduced into $\sigma_{\max}\left(\left(\mathbf{E}_{qr,\mathcal{I}}\mathbf{\Pi}_{qr,\mathcal{I}}\right)^{+}\mathbf{G}_{qr,\mathcal{I}}\left(\mathbf{x}_{-q}\right)\right)$ without modifying its value. Using standard matrix theoretic properties for partitioned matrices, the projector $\mathbf{\Pi}_{qr,\mathcal{I}}$ is obtained as

$$\mathbf{\Pi}_{qr,\mathcal{I}} = \begin{bmatrix} \mathbf{0}_{N\times N} & \mathbf{0}_{N\times m} \\ \mathbf{0}_{m\times n} & \mathbf{I}_m - \frac{\mathbf{1}_m\mathbf{1}_m^\top}{m} \end{bmatrix}.$$

Letting $\xi_{qr} \triangleq \frac{R_{\mathrm{up},q}}{\prod_{p\neq q}(1-\mathbb{P}_p+\mathbb{P}_p x_{p,0})} \frac{\mathbb{P}_r}{(1-\mathbb{P}_r+\mathbb{P}_r x_{r,0})}$, this leads to

$$\left(\mathbf{E}_{qr,\mathcal{I}}\mathbf{\Pi}_{qr,\mathcal{I}}\right)^{+}\mathbf{G}_{qr,\mathcal{I}}\left(\mathbf{x}_{-q}\right) = \frac{\xi_{qr}}{\left\|\left(\mathbf{I}_m - \frac{\mathbf{1}_m\mathbf{1}_m^\top}{m}\right)\mathbf{w}_{q,\mathcal{I}^{\mathrm{Na}}}\right\|_2^2} \begin{bmatrix} \mathbf{0}_N & \mathbf{0}_{N\times A_r} \\ -\left(\mathbf{I}_m - \frac{\mathbf{1}_m\mathbf{1}_m^\top}{m}\right)\mathbf{w}_{q,\mathcal{I}^{\mathrm{Na}}} & \mathbf{0}_{m\times A_r} \end{bmatrix},$$

whose maximum singular value is obtained as

$$\begin{aligned} \sigma_{\max}\left(\left(\mathbf{E}_{qr,\mathcal{I}}\mathbf{\Pi}_{qr,\mathcal{I}}\right)^{+}\mathbf{G}_{qr,\mathcal{I}}\left(\mathbf{x}_{-q}\right)\right) &= \frac{\xi_{qr}}{\left\|\left(\mathbf{I}_m - \frac{\mathbf{1}_m\mathbf{1}_m^\top}{m}\right)\mathbf{w}_{q,\mathcal{I}^{\mathrm{Na}}}\right\|_2}, \\ &= \frac{\xi_{qr}}{\sqrt{\sum_{i\in\mathcal{I}^{\mathrm{Na}}} w_{q,i}^2 - \frac{\left(\sum_{i\in\mathcal{I}^{\mathrm{Na}}} w_i\right)^2}{m}}}. \end{aligned} \tag{21}$$

It remains to maximise the above with respect to the other players strategies, and to the constraint sets. For this latter, it is noticed that by removing a index i_0 from $\mathcal{I}^{\mathrm{Na}}$, the above quantity never decreases:

$$\begin{aligned} &\sum_{i\in\mathcal{I}^{\mathrm{Na}}} w_{q,i}^2 - \frac{\left(\sum_{i\in\mathcal{I}^{\mathrm{Na}}} w_i\right)^2}{m} \\ &\qquad - \sum_{i\in\mathcal{I}^{\mathrm{Na}}\setminus\{i_0\}} w_{q,i}^2 - \frac{\left(\sum_{i\in\mathcal{I}^{\mathrm{Na}}\setminus\{i_0\}} w_i\right)^2}{m-1} \\ &\qquad = \frac{\left(\sum_{i\in\mathcal{I}^{\mathrm{Na}}\setminus\{i_0\}} w_{q,i} - (m-1)\, w_{q,i_0}\right)^2}{m\,(m-1)}. \end{aligned}$$

Thus, the smallest sets $\mathcal{I}^{\mathrm{Na}}$ must be considered, being at least of size 2 since $m = A_q + 2 - |\mathcal{I}| \geq 2$ for linearly independent constraint sets. Moreover, for sets with two elements, it can be observed that consecutive $w_{q,i}$'s will lead to the maximum of (21), if the $w_{q,i}$'s are sorted. In that case, the convergence matrix elements are obtained as

$$\left[\mathbf{\Gamma}^{\mathrm{cons}}\right]_{qr} \triangleq \frac{R_{\mathrm{up},q}}{\prod_{p\neq q}\left(1-\mathbb{P}_p x_p^{\max}\right)} \frac{\mathbb{P}_r}{\left(1-\mathbb{P}_r x_r^{\max}\right)} \frac{\sqrt{2}}{\min_{i=0,\ldots,A_q-1}\left|w_{q,i}-w_{q,i+1}\right|}.$$

To conclude the convergence analysis, it is noticed that $\rho\left(\mathbf{\Gamma}\right) = \rho\left(\mathbf{T}\mathbf{\Gamma}\mathbf{T}^{-1}\right)$ whatever the invertible matrix $\mathbf{T}$ [55, Fact 4.45.xii], and that the desired expression is obtained with $\mathbf{T} = \mathrm{Diag}\left(\left[\frac{\mathbb{P}_1}{1-\mathbb{P}_1 x_1^{\max}}, \ldots, \frac{\mathbb{P}_Q}{1-\mathbb{P}_Q x_Q^{\max}}\right]\right)$.

REFERENCES

[1] C. Zhang, Y. Xie, H. Bai, B. Yu, W. Li, and Y. Gao, "A survey on federated learning," *Knowledge-Based Systems*, vol. 216, p. 106775, 2021. [Online]. Available: https://www.sciencedirect.com/science/article/pii/S0950705121000381

[2] W. Y. B. Lim, N. C. Luong, D. T. Hoang, Y. Jiao, Y.-C. Liang, Q. Yang, D. Niyato, and C. Miao, "Federated learning in mobile edge networks: A comprehensive survey," *IEEE Communications Surveys & Tutorials*, vol. 22, no. 3, pp. 2031–2063, 2020.

[3] G. Scutari, F. Facchinei, J.-S. Pang, and D. P. Palomar, "Real and complex monotone communication games," *IEEE Transactions on Information Theory*, vol. 60, no. 7, pp. 4197–4231, 2014.

[4] F. Facchinei and C. Kanzow, "Generalized nash equilibrium problems," *Annals of Operations Research*, vol. 175, no. 1, pp. 177–211, 2010.

[5] L. Qian, P. Yang, M. Xiao, O. A. Dobre, M. D. Renzo, J. Li, Z. Han, Q. Yi, and J. Zhao, "Distributed learning for wireless communications: Methods, applications and challenges," *IEEE Journal of Selected Topics in Signal Processing*, vol. 16, no. 3, pp. 326–342, 2022.

[6] S. Zheng, C. Shen, C. Shen, X. Chen, and X. Chen, "Design and analysis of uplink and downlink communications for federated learning," *IEEE Journal on Selected Areas in Communications*, 2020.

[7] Y.-J. Liu, S. Qin, Y. Sun, and G. Feng, "Resource consumption for supporting federated learning in wireless networks," *IEEE Transactions on Wireless Communications*, vol. 21, no. 11, pp. 9974–9989, 2022.

[8] C. T. Dinh, N. H. Tran, M. N. H. Nguyen, M. N. H. Nguyen, M. N. H. Nguyen, C. S. Hong, W. Bao, A. Y. Zomaya, A. Y. Zomaya, A. Y. Zomaya, A. Y. Zomaya, and V. Gramoli, "Federated learning over wireless networks: Convergence analysis and resource allocation." *arXiv: Learning*, 2019.

[9] V.-D. Nguyen, S. K. Sharma, T. X. Vu, S. Chatzinotas, S. Chatzinotas, and B. Ottersten, "Efficient federated learning algorithm for resource allocation in wireless iot networks," *IEEE Internet of Things Journal*, 2020.

[10] Y. Wu, Y. Song, T. Wang, L. Qian, and T. Q. Quek, "Non-orthogonal multiple access assisted federated learning via wireless power transfer: A cost-efficient approach," *IEEE Transactions on Communications*, 2022.

[11] Z. Yang, M. Chen, W. Saad, C. S. Hong, and M. Shikh-Bahaei, "Energy efficient federated learning over wireless communication networks," *IEEE Transactions on Wireless Communications*, vol. 20, no. 3, pp. 1935–1949, 2021.

[12] N. H. Tran, W. Bao, A. Zomaya, M. N. H. Nguyen, and C. S. Hong, "Federated learning over wireless networks: Optimization model design and analysis," in *IEEE INFOCOM 2019 - IEEE Conference on Computer Communications*, 2019, pp. 1387–1395.

[13] W. Shi, S. Zhou, Z. Niu, M. Jiang, and L. Geng, "Joint device scheduling and resource allocation for latency constrained wireless federated learning," *IEEE Transactions on Wireless Communications*, 2020.

[14] S. Wang, T. Tuor, T. Salonidis, K. K. Leung, C. Makaya, T. He, K. S. Chan, and K. S. Chan, "Adaptive federated learning in resource constrained edge computing systems," *IEEE Journal on Selected Areas in Communications*, 2019.

[15] S. M. I. H. Chen, S. Huang, D. Zhang, F. I. M. Skoglund, L. F. I. H. V. Poor, H. Chen, and M. Xiao, "Federated learning over wireless iot networks with optimized communication and resources," *IEEE Internet of Things Journal*, 2021.

[16] D. Liu and O. Simeone, "Privacy for free: Wireless federated learning via uncoded transmission with adaptive power control," *IEEE Journal on Selected Areas in Communications*, 2021.

[17] R. Gupta and J. Gupta, "Federated learning using game strategies: State-of-the-art and future trends," *Comput. Networks*, 2023.

[18] X. Tu, K. Zhu, N. C. Luong, D. Niyato, Y. Zhang, and J. Li, "Incentive mechanisms for federated learning: From economic and game theoretic perspective," *IEEE Transactions on Cognitive Communications and Networking*, 2021.

[19] A. Richardson, A. Filos-Ratsikas, and B. Faltings, "Budget-bounded incentives for federated learning," *Federated Learning: Privacy and Incentive*, pp. 176–188, 2020.

© 2024 IEEE. Personal use is permitted, but republication/redistribution requires IEEE permission. See https://www.ieee.org/publications/rights/index.html for more information.

This article has been accepted for publication in IEEE Internet of Things Journal. This is the author's version which has not been fully edited and content may change prior to final publication. Citation information: DOI 10.1109/JIOT.2024.3364756

[20] G. Huang, X. Chen, T. Ouyang, Q. Ma, L. Chen, and J. Zhang, "Collaboration in participant-centric federated learning: A game-theoretical perspective," *IEEE Transactions on Mobile Computing*, pp. 1–16, 2022.

[21] C. W. Zaw, S. R. Pandey, K. Kim, and C. S. Hong, "Energy-aware resource management for federated learning in multi-access edge computing systems," *IEEE Access*, 2021.

[22] C. W. Zaw and C. S. Hong, "A decentralized game theoretic approach for energy-aware resource management in federated learning," *International Conference on Big Data and Smart Computing*, 2021.

[23] H. Althumali and M. Othman, "A survey of random access control techniques for machine-to-machine communications in lte/lte-a networks," *IEEE Access*, vol. 6, pp. 74 961–74 983, 2018.

[24] C.-H. Chang and R. Y. Chang, "Design and analysis of multichannel slotted aloha for machine-to-machine communication," in *2015 IEEE Global Communications Conference (GLOBECOM)*, 2015, pp. 1–6.

[25] N. Tian, C. Li, J. Cheng, W. Yue, and M. Luo, "Decentralized power control for an aloha-type random multiple access system with short packet transmission," *Wireless Communications and Mobile Computing*, vol. 2022, 2022.

[26] E. Balevi, F. T. A. Rabee, and R. D. Gitlin, "Aloha-noma for massive machine-to-machine iot communication," in *2018 IEEE International Conference on Communications (ICC)*, 2018, pp. 1–5.

[27] C. Sun, S. Ma, C. Zheng, S. Wu, T. Cui, and L. Lyu, "Federated learning over a wireless network: Distributed user selection through random access," *arXiv preprint arXiv:2307.03758*, 2023.

[28] A. Salama, A. Stergioulis, A. M. Hayajneh, S. A. R. Zaidi, D. McLernon, and I. Robertson, "Decentralized federated learning over slotted aloha wireless mesh networking," *IEEE Access*, vol. 11, pp. 18 326–18 342, 2023.

[29] H. Han, J. Zhao, and X. Zhou, "A random access scheme for federated learning over massive mimo systems," *IEEE Internet of Things Journal*, vol. 10, no. 21, pp. 19 027–19 042, 2023.

[30] J. Choi and S. R. Pokhrel, "Federated learning with multichannel aloha," *IEEE Wireless Communications Letters*, vol. 9, no. 4, pp. 499–502, 2019.

[31] R. V. da Silva, J. Choi, J. Park, G. Brante, and R. D. Souza, "Multichannel aloha optimization for federated learning with multiple models," *IEEE Wireless Communications Letters*, vol. 11, no. 10, pp. 2180–2184, 2022.

[32] R. V. Da Silva, O. L. A. López, and R. D. Souza, "Energy-aware federated learning with distributed user sampling and multichannel aloha," *IEEE Communications Letters*, 2023.

[33] G. Debreu, "A social equilibrium existence theorem," *Proceedings of the National Academy of Sciences*, vol. 38, no. 10, pp. 886–893, 1952.

[34] K. J. Arrow and G. Debreu, "Existence of an equilibrium for a competitive economy," *Econometrica: Journal of the Econometric Society*, pp. 265–290, 1954.

[35] C. Dutang, "A survey of gne computation methods: theory and algorithms," 2013.

[36] A. Fischer, M. Herrich, and K. Schönefeld, "Generalized nash equilibrium problems-recent advances and challenges," *Pesquisa Operacional*, vol. 34, no. 3, pp. 521–558, 2014.

[37] F. Facchinei and S. Sagratella, "On the computation of all solutions of jointly convex generalized nash equilibrium problems," *Optimization Letters*, vol. 5, no. 3, pp. 531–547, 2011.

[38] A. Dreves, F. Facchinei, C. Kanzow, and S. Sagratella, "On the solution of the kkt conditions of generalized nash equilibrium problems," *SIAM Journal on Optimization*, vol. 21, no. 3, pp. 1082–1108, 2011.

[39] F. Facchinei, C. Kanzow, and S. Sagratella, "Solving quasi-variational inequalities via their kkt conditions," *Mathematical Programming*, vol. 144, no. 1, pp. 369–412, 2014.

[40] J.-S. Pang and M. Fukushima, "Quasi-variational inequalities, generalized nash equilibria, and multi-leader-follower games," *Computational Management Science*, vol. 2, pp. 21–56, 2005.

[41] F. Facchinei, A. Fischer, and V. Piccialli, "Generalized nash equilibrium problems and newton methods," *Mathematical Programming*, vol. 117, no. 1-2, pp. 163–194, 2009.

[42] A. Singh and D. Ghosh, "A globally convergent improved bfgs method for generalized nash equilibrium problems," *SeMA Journal*, pp. 1–27, 2023.

[43] F. Facchinei and C. Kanzow, "Penalty methods for the solution of generalized nash equilibrium problems," *SIAM Journal on Optimization*, vol. 20, no. 5, pp. 2228–2253, 2010.

[44] T. Migot and M.-G. Cojocaru, "A decomposition method for a class of convex generalized nash equilibrium problems," *Optimization and Engineering*, vol. 22, pp. 1653–1679, 2021.

[45] J. G. Kim, "Equilibrium computation of generalized nash games: A new lagrangian-based approach," *arXiv preprint arXiv:2106.00109*, 2021.

[46] I. Stupia, L. Sanguinetti, G. Bacci, and L. Vandendorpe, "Power control in networks with heterogeneous users: A quasi-variational inequality approach," *IEEE Transactions on Signal Processing*, vol. 63, no. 21, pp. 5691–5705, 2015.

[47] J.-S. Pang, G. Scutari, F. Facchinei, and C. Wang, "Distributed power allocation with rate constraints in gaussian parallel interference channels," *IEEE Transactions on Information Theory*, vol. 54, no. 8, pp. 3471–3489, 2008.

[48] G. Thiran, I. Stupia, and L. Vandendorpe, "Energy efficient competitive resource allocation in mimo networks," *arXiv preprint arXiv:2012.07312*, 2020.

[49] F. Facchinei, V. Piccialli, and M. Sciandrone, "Decomposition algorithms for generalized potential games," *Computational Optimization and Applications*, vol. 50, no. 2, pp. 237–262, 2011.

[50] J. Nie, X. Tang, and L. Xu, "The gauss–seidel method for generalized nash equilibrium problems of polynomials," *Computational Optimization and Applications*, vol. 78, pp. 529–557, 2021.

[51] T. Nishio and R. Yonetani, "Client selection for federated learning with heterogeneous resources in mobile edge," in *ICC 2019-2019 IEEE international conference on communications (ICC)*. IEEE, 2019, pp. 1–7.

[52] H. H. Yang, Z. Liu, T. Q. S. Quek, and H. V. Poor, "Scheduling policies for federated learning in wireless networks," *IEEE Transactions on Communications*, vol. 68, no. 1, pp. 317–333, 2020.

[53] J. P. Boyle and R. L. Dykstra, "A method for finding projections onto the intersection of convex sets in hilbert spaces," in *Advances in Order Restricted Statistical Inference*, R. Dykstra, T. Robertson, and F. T. Wright, Eds. New York, NY: Springer New York, 1986, pp. 28–47.

[54] D. Bertsekas and J. Tsitsiklis, "Parallel and distributed computation : numerical methods / Dimitri P. Bertsekas, John N. Tsitsiklis," *SERBIULA (sistema Librum 2.0)*, 1989.

[55] D. S. Bernstein, *Matrix mathematics*. Princeton university press, 2009.

[56] S. Boyd, S. P. Boyd, and L. Vandenberghe, *Convex optimization*. Cambridge university press, 2004.

[57] H. Whitney, "Analytic extensions of differentiable functions defined in closed sets," *Hassler Whitney Collected Papers*, pp. 228–254, 1992.

[58] S. M. Robinson, "Stability theory for systems of inequalities. part i: Linear systems," *SIAM Journal on Numerical Analysis*, vol. 12, no. 5, pp. 754–769, 1975.

[59] D. P. Bertsekas, "Nonlinear programming," *Journal of the Operational Research Society*, vol. 48, no. 3, pp. 334–334, 1997.

[60] G. Giorgi *et al.*, "A guided tour in constraint qualifications for nonlinear programming under differentiability assumptions," University of Pavia, Department of Economics and Management, Tech. Rep., 2018.

[61] R. Janin, "Directional derivative of the marginal function in nonlinear programming," in *Sensitivity, Stability and Parametric Analysis*. Springer, 1984, pp. 110–126.

[62] J. Liu, "Sensitivity analysis in nonlinear programs and variational inequalities via continuous selections," *SIAM Journal on Control and Optimization*, vol. 33, no. 4, pp. 1040–1060, 1995.

[63] J. E. Spingarn and R. T. Rockafellar, "The generic nature of optimality conditions in nonlinear programming," *Mathematics of Operations Research*, vol. 4, no. 4, pp. 425–430, 1979.

[64] A. V. Fiacco *et al.*, *Introduction to sensitivity and stability analysis in nonlinear programming*. Academic press, 1983, vol. 165.

[65] F. H. Clarke, "Generalized gradients of lipschitz functionals," *Advances in Mathematics*, vol. 40, no. 1, pp. 52–67, 1981.

[66] ——, *Optimization and nonsmooth analysis*. SIAM, 1990.

[67] R. T. Rockafellar and R. J.-B. Wets, *Variational analysis*. Springer Science & Business Media, 2009, vol. 317.

© 2024 IEEE. Personal use is permitted, but republication/redistribution requires IEEE permission. See https://www.ieee.org/publications/rights/index.html for more information.